CHAPTER 1

INTRODUCTION TO SELF-EXCITED DYNAMO ACTION

Benoît Desjardins, Emmanuel Dormy
Andrew Gilbert & Michael Proctor.

The theory of self-excited dynamo action discussed throughout this volume was first suggested by Sir Joseph Larmor in 1919 to account for the magnetic field of sunspots. It was later formalised mathematically by Walter Elsasser (1946). The objective of this first chapter is to introduce the subject and provide the necessary background for the later developments. We derive the relevant equations and discuss the usual approximations in Section 1.1. The concept of a homogeneous self-excited dynamo is introduced in Section 1.2. The existing theoretical results and necessary conditions for dynamo action are then presented Section 1.3, and the essential distinction between steady and time-dependent velocities is made in Section 1.4. We then introduce mean field electromagnetism (a continuing theme throughout the book) in Section 1.4 and the difficult large magnetic Reynolds number limit (relevant to astrophysical problems) in Section 1.6.

1.1. GOVERNING EQUATIONS

1.1.1. MAGNETIC INDUCTION

The common aspect among all natural objects described in this volume is their ability to maintain their own magnetic field. This is described by the induction equation

which we shall derive now.

We will deal with a variety of conducting fluids ranging from molten iron in the Earth's core to ionized gas in stars and galaxies. Yet the magnetic field in these objects is usually well defined by the so called induction equation.

INDUCTION EQUATION

Let us first recall Maxwell's equations

$$\boldsymbol{\nabla} \times \mathbf{E} = -\partial_t \mathbf{B}\,, \qquad \boldsymbol{\nabla} \times \mathbf{B} = \mu\,\mathbf{j} + \varepsilon\,\mu\,\partial_t \mathbf{E}\,, \tag{1.1a,b}$$

$$\boldsymbol{\nabla} \cdot \mathbf{B} = 0\,, \qquad \boldsymbol{\nabla} \cdot \mathbf{E} = \rho_c/\varepsilon\,, \tag{1.1c,d}$$

where the following notation $\partial_t \cdot \equiv \partial \cdot / \partial t$ has been used. $\mathbf{B}$ is the magnetic induction (sometimes refered to as the magnetic field), $\mathbf{E}$ is the electric field, $\mathbf{j}$ is the electric current density, ρ_c is the charge density, μ is the magnetic permeability, ε the dielectric constant. In the following we will assume the free-space value for the magnetic permeability $\mu \simeq \mu_o = 4\pi \times 10^{-7}$ and $\varepsilon \simeq \varepsilon_o = (\mu_o c^2)^{-1}$, then (1.1b) can be rewritten

$$\boldsymbol{\nabla} \times \mathbf{B} = \mu\,\mathbf{j} + c^{-2}\,\partial_t \mathbf{E}\,, \tag{1.2}$$

the last term can obviously be neglected provided the typical velocity of the phenomena we investigate (i.e. the ratio of a typical length scale to a typical time) remains small compared to the speed of light c. We will therefore neglect this term in the sequel, on the basis of a "low-frequency" approximation,

$$\boldsymbol{\nabla} \times \mathbf{B} = \mu\,\mathbf{j}\,. \tag{1.3}$$

An additional constitutive relation is required, it is Ohm's law relating electric currents to the electric field throught the electrical conductivity σ

$$\mathbf{j} = \sigma \mathbf{E}\,. \tag{1.4}$$

These equations are valid in a reference frame at rest. Because the fluids we will consider are generally not at rest, it is necessary to introduce some modifications for the equations to be valid in the case of a moving medium. Following standard electromagnetic theory

$$\begin{cases} \mathbf{E}' = (1-\gamma_u)\,\dfrac{\mathbf{u}\cdot\mathbf{E}}{|\mathbf{u}|^2}\,\mathbf{u} + \gamma_u\,(\mathbf{E} + \mathbf{u}\times\mathbf{B})\,, \\ \mathbf{B}' = (1-\gamma_u)\,\dfrac{\mathbf{u}\cdot\mathbf{B}}{|\mathbf{u}|^2}\,\mathbf{u} + \gamma_u\left(\mathbf{B} - \dfrac{\mathbf{u}\times\mathbf{E}}{c^2}\right)\,, \end{cases} \tag{1.5a,b}$$

where $\gamma_u = (1 - |\mathbf{u}|^2/c^2)^{-1/2}$ is the Lorentz factor.

Under the assumption that $|\,\mathbf{u}\,| \ll c$, the Lorentz factor can be set equal to unity. From (1.1a), it follows that $|\,\mathbf{E}\,| \sim |\,\mathbf{u}\,|\,|\,\mathbf{B}\,|$, and the only modification associated with the displacement of the reference frame is therefore

$$\mathbf{E}' = \mathbf{E} + \mathbf{u} \times \mathbf{B}\,, \tag{1.6}$$

and Ohm's law then becomes

$$\mathbf{j} = \sigma\,(\mathbf{E} + \mathbf{u} \times \mathbf{B})\ . \tag{1.7}$$

Let us now assume that the medium is in neutral state, more explicitly

$$\rho_c \equiv Z_i\, n_i - e\, n_e = 0\,, \tag{1.8}$$

where ρ_c is the charge density Z_i is the average charge of ions in the medium, and n_e and n_i are the number densities respectively of free electrons and ions.

As stressed by Roberts (1967), this assumption cannot be rigorously valid in a fluid conductor, since the divergence of (1.7) with (1.1d) implies

$$\boldsymbol{\nabla} \cdot (\mathbf{u} \times \mathbf{B}) = -\rho_c/\varepsilon \tag{1.9}$$

Because $\boldsymbol{\nabla} \cdot (\mathbf{u} \times \mathbf{B}) \neq 0$ the charge density cannot be exactly vanishing. One can however rely again on the smallness of ε to neglect ρ_c in the sequel.

Electrical currents are present in the medium provided $\mathbf{u}_e \neq \mathbf{u}_i$, then

$$\mathbf{j} = Z_i\, n_i\, \mathbf{u}_i - e\, n_e\, \mathbf{u}_e\,, \tag{1.10}$$

using (1.8) $$\mathbf{j} = -e\, n_e\, \mathbf{u}'_e\,,\ \text{with}\ \mathbf{u}'_e = \mathbf{u}_e - \mathbf{u}_i\,. \tag{1.11}$$

From a strict point of view, the three equations of motion should now be established, one for each: neutrals, ions and electrons.

The key assumption in single-fluid MHD is that collisions occur often enough to mechanically couple all three components. We need in particular to formulate this assumption for ions and neutrals. In fact, while this is clearly a valid assumption for the Earth's core or for solar dynamics, in some weakly ionized plasmas relevant to the interstellar medium (ISM), the drift of charged particles with respect to the neutrals can become significant. This effect is referred to as ambipolar drift, or ambipolar diffusion.[1] We will not consider this effect at this stage.

1 The term "ambipolar diffusion" can be slightly misleading, since this effect is not strictly equivalent to resistive diffusion. In particular, it preserves magnetic topology (as will be discussed later for ideal MHD). Still, this effect acts to damp fluctuations on small scales.

The relative velocity of electrons to ions, $\mathbf{u}'_e$, can be estimated from the amplitude necessary to produce electrical currents compatible with the observed magnetic fields for the geophysical and astrophysical applications addressed in this book.

From (1.3) and (1.11) we write

$$|\,\mathbf{u}'_e\,| \simeq \frac{|\,\mathbf{B}\,|}{\mu\, L\ |e|\ n_e}\,, \tag{1.12}$$

which can be used to obtain rough estimates of $\mathbf{u}'_e$:

– in the case of the Earth's core

$$|\,\mathbf{u}'_e\,| \simeq \frac{10^{-4}}{4\pi \times 10^{-7} \times 10^{6} \times 2 \times 10^{-19} \times 10^{29}} \simeq 10^{-20}\mathrm{m\,s^{-1}}\,. \tag{1.13a}$$

– in the case of the Sun

$$|\,\mathbf{u}'_e\,| \simeq \frac{10^{-1}}{4\pi \times 10^{-7} \times 2 \times 10^{8} \times 2 \times 10^{-19} \times 10^{29}} \simeq 10^{-14}\mathrm{m\,s^{-1}}\,. \tag{1.13b}$$

– in the case of galaxies

$$|\,\mathbf{u}'_e\,| \simeq \frac{5 \times 10^{-10}}{4\pi \times 10^{-7} \times 10^{20} \times 2 \times 10^{-19} \times 10^{3}} \simeq 10^{-8}\mathrm{m\,s^{-1}}\,. \tag{1.13c}$$

In all these cases the velocity of the flow $|\ \mathbf{u}\ |$ (i.e. ions and neutrals) is much larger than $|\,\mathbf{u}'_e\,|$. $|\,\mathbf{u}\,|$ is of the order of $10^{-4}\mathrm{m\,s^{-1}}$ in the slow moving liquid iron Earth's core, and much larger in the Sun and in galaxies. These are thus extremely small deviations from the mean velocity. We shall therefore adopt the "single fluid" approximation, i.e. we will assume $\mathbf{u}_n \simeq \mathbf{u}_i \simeq \mathbf{u}_e$ and use a single fluid model, while retaining the small difference $\mathbf{u}'_e = \mathbf{u}_e - \mathbf{u}_i$ only as a source of magnetic induction.

The curl of (1.7), with (A.25) and (1.1c), immediately yields,

$$\partial_t \mathbf{B} = \boldsymbol{\nabla} \times (\mathbf{u} \times \mathbf{B}) + \eta\, \Delta \mathbf{B}\,, \qquad (\text{where } \Delta \equiv \boldsymbol{\nabla}^2)\,, \tag{1.14}$$

the coefficient $\eta = 1/(\sigma\,\mu)$ is referred to as the *magnetic diffusivity*, assumed here to be constant. One must not forget the additional constraint provided by (1.1c):

$$\boldsymbol{\nabla} \cdot \mathbf{B} = 0\,. \tag{1.15}$$

It is to be noted that, provided this constraint is satified at a given time, (1.14) will ensure it remains satisfied for all time.

In addition, this constraint can conveniently be used to rewrite the magnetic field in terms of a vector potential $\mathbf{A}$

$$\mathbf{B} = \boldsymbol{\nabla} \times \mathbf{A}\,. \tag{1.16}$$

INFLUENCE ON MATTER

We have seen above how fluid motions can affect the magnetic induction. The induction equation derived above is the starting point of dynamo theory. However with this equation alone, and a prescribed flow, the field is governed by a linear equation (this is referred to as the "kinematic dynamo" problem, and will be discussed later in this chapter). The magnetic field could then grow exponentially and reach unrealistic values. In fact a retroaction of the field on the flow, in the form of the Lorentz force, prevents such accidents.

The Lorentz force density is given by

$$F_L = n_i Z_i \left(E + \mathbf{u}_i \times \mathbf{B}\right) - n_e e \left(E + \mathbf{u}_e \times \mathbf{B}\right) = \mathbf{j} \times \mathbf{B} = {\mu_0}^{-1} (\boldsymbol{\nabla} \times \mathbf{B}) \times \mathbf{B}\,, \tag{1.17}$$

where (1.8) and (1.10) have been used. This force density applies to the single-fluid described above. It can be expended as

$${\mu_0}^{-1} (\boldsymbol{\nabla} \times \mathbf{B}) \times \mathbf{B} = {\mu_0}^{-1} \left[(\mathbf{B} \cdot \boldsymbol{\nabla}) \mathbf{B} - \tfrac{1}{2} \boldsymbol{\nabla} \left| \mathbf{B} \right|^2 \right] , \tag{1.18}$$

where the first term is known as the "magnetic tension", and the second as the "magnetic pressure".

1.1.2. THERMODYNAMIC EQUATIONS

In the case of planets and stars, it is expected that convection is the main source of motions. We will assume, for simplicity, a single driving mechanism for convection in this section. This is not fully valid for investigating the Earth's core, for which compositional as well as thermal driving need to be considered. A similar set of equations can however be recovered in this case by introducing a codensity variable accounting for both of these effects. For a rigorous derivation of the equations in this more complicated case and including turbulence modelling, the reader should refer to Braginsky and Roberts (1995, 2003).

Denoting by P, ρ and T, the pressure, density and temperature, we assume that the equation of state of the fluid is given by the following three thermodynamic coefficients, the dilatation coefficient for constant pressure α_P, the specific heat at constant pressure c_P, and the polytropic coefficient γ :

$$\alpha_P = -\frac{T}{\rho} \frac{\partial \rho}{\partial T}\bigg|_P , \qquad c_P = \frac{\partial H}{\partial T}\bigg|_P , \qquad \gamma = \frac{\rho}{P} \frac{\partial P}{\partial \rho}\bigg|_S , \tag{1.19a,b,c}$$

where H denotes the specific enthalpy, and S denotes the specific entropy of the system.

From the second principle of Thermodynamics, we deduce that

$$\mathrm{d}E = T\mathrm{d}S + \frac{P}{\rho^2}\mathrm{d}\rho\,, \tag{1.20}$$

where $E = H - P/\rho$ denotes the specific internal energy, and thus

$$c_P = T\left.\frac{\partial S}{\partial T}\right|_P. \tag{1.21}$$

Finally, one can also introduce for convenience

$$\alpha_S = -\frac{1}{\rho}\left.\frac{\partial \rho}{\partial S}\right|_P = \frac{\alpha_P}{c_P}\,. \tag{1.22}$$

All thermodynamic relations are deduced from (1.20) and the preceding three coefficients. Indeed, from (1.20)

$$\frac{\mathrm{d}P}{P}\left(\frac{1}{\gamma} + \frac{P\alpha_P^2}{\rho T c_P}\right) = \frac{\mathrm{d}\rho}{\rho} + \frac{\alpha_P \mathrm{d}T}{T}\,, \tag{1.23a}$$

$$\frac{\mathrm{d}S}{c_P} = \frac{\mathrm{d}T}{T} - \frac{P\alpha_P}{\rho T c_P}\frac{\mathrm{d}P}{P}\,, \tag{1.23b}$$

and

$$\alpha_S \mathrm{d}S = \frac{1}{\gamma}\frac{\mathrm{d}P}{P} - \frac{\mathrm{d}\rho}{\rho}\,. \tag{1.23c}$$

Introducing the heat production δQ, the heat flux $\mathbf{q}$, and the rate of internal dissipation per unit volume $\mathcal{E}$ (including viscous and ohmic dissipation), we can rewrite the second principle of Thermodynamics, using the fact that $T\mathrm{d}S = \delta Q = -\boldsymbol{\nabla}\cdot\mathbf{q}$

$$\rho\,\mathrm{D}_t E - \frac{p}{\rho}\mathrm{D}_t\rho = -\boldsymbol{\nabla}\cdot\mathbf{q} + \mathcal{E}\,, \qquad \text{where} \qquad \mathrm{D}_t \equiv \partial_t + \mathbf{u}\cdot\boldsymbol{\nabla} \tag{1.24a,b}$$

denotes the lagrangian derivative.

This expression, together with Fourier's law of heat conduction for the temperature T (introducing the thermal conduction coefficient k)

$$\mathbf{q} = -k\boldsymbol{\nabla}T\,, \qquad \text{yields} \qquad \rho\,T\,\mathrm{D}_t S = \boldsymbol{\nabla}\cdot(k\boldsymbol{\nabla}T) + \mathcal{E}\,. \tag{1.25a,b}$$

1.1.3. NAVIER-STOKES EQUATION

The compressible Navier-Stokes equations include the continuity equation,

$$\partial_t\rho + \boldsymbol{\nabla}\cdot(\rho\,\mathbf{u}) = 0\,, \qquad \text{or} \qquad D_t\rho = -\rho\,\boldsymbol{\nabla}\cdot\mathbf{u}\,, \tag{1.26a,b}$$

and the momentum equation, written in a rotating reference frame

$$\rho D_t \mathbf{u} + 2\,\rho\,\mathbf{\Omega} \times \mathbf{u} = -\boldsymbol{\nabla} P - \rho\,\boldsymbol{\nabla}\Phi - \boldsymbol{\nabla}\cdot\boldsymbol{\tau} + \mathcal{F}\,, \tag{1.26c}$$

where $\mathcal{F}$ represents the remaining body forces (including the Lorentz force), and $\boldsymbol{\tau}$ is the viscous stress tensor, with components

$$\tau_{ij} = -2\rho\nu s_{ij}\,, \qquad s_{ij} = \varepsilon_{ij} - \tfrac{1}{3}\,(\boldsymbol{\nabla}\cdot\mathbf{u})\,\delta_{ij}\,, \tag{1.26d,e}$$

ν being the kinematic viscosity, S_{ij} the strain rate tensor

$$S_{ij} = \tfrac{1}{2}\left(\partial_i u_j + \partial_j u_i\right)\,, \tag{1.26f}$$

and Φ includes the gravity potential Φ_g and the centrifugal potential Φ_Ω.

The apparent gravity field is then provided by $\mathbf{g} = -\boldsymbol{\nabla}\Phi$. There are here two contributions to Φ. In a non rotating problem, the gravity potential is simply obtained from

$$\Delta\Phi_g = 4\pi G\rho\,. \tag{1.27}$$

In a rotating fluid, this potential is complemented by the effect of the centrifugal potential

$$\Phi_\Omega = \frac{\Omega^2 s^2}{2}\,, \qquad\qquad \Delta\Phi_\Omega = -2\Omega^2\,. \tag{1.28a,b}$$

For a galactic disk, density is low and centrifugal effects are essential. They balance the radial component of gravity. As a result, the apparent gravity is oriented along the axis of rotation.

For much denser objects, like the Earth or the Sun, the *rôle* of the centrifugal effect is much smaller. It essentially flattens equipotential surfaces. This effect is minute for these objects, which are almost spherical bodies. Under this assumtion, gravity potential varies only with radius. On a given sphere of radius r, and outward normal $\mathbf{n}$:

$$\int_{S(r)} \boldsymbol{\nabla}\Phi\cdot\mathbf{n}\,\mathrm{d}S = 4\pi\,G\int_{V(r)}\rho\,\mathrm{d}V\,, \tag{1.29}$$

masses at larger radii cancel their contributions. So that for a sphere of uniform density, gravity is proportionnal to radius:

$$\mathbf{g} = -\tfrac{4}{3}\pi G\rho r\,\mathbf{e}_r. \tag{1.30}$$

Note that using (1.26a,b), the energy equations (1.24a) can be rewritten as

$$\rho\,\mathrm{D}_t E + P\,\boldsymbol{\nabla}\cdot\mathbf{u} = \boldsymbol{\nabla}\cdot(k\boldsymbol{\nabla}T) + \mathcal{E}\,. \tag{1.31}$$

These equations need to be complemented by an equation of state relating P, ρ, and T as described in the previous section.

This set of equations is appropriate to describe the dynamics of galaxies. Simpler models can however be derive for convection in planets and stars. This is the objects of the next section.

ANELASTIC APPROXIMATION

Two major steps constitute the anelastic approximation. The first consists in filtering out acoustic waves, while the second is a linearization of fluctuating variables around the reference state. Both can be achieved by an appropriate expansion.

In order to derive the most classical approximated models, we rewrite the above set of equations in dimensionless form. Let us introduce a typical velocity U_*, length L_*, density ρ_*, and temperature T_*. Equation (1.23b) provides $P_* = \rho_* T_* c_{p_*}/\alpha_{p_*} = \rho_* T_*/\alpha_{s*}$. Having set four units, and since nine parameters define our problem $(L, T_*, \rho_*, c_{p_*}, \alpha_{p_*}, \nu, k, G, \Omega)$, five independant non-dimensional combinations can be constructed. We define the Reynolds number Re, the Rossby number Ro (mesuring the ratio between the rotation and the hydrodynamic time scale), the Froude number Fr (mesuring inertia versus gravity forces), the ratio $\mathcal{X}$ of gravity to pressure forces, and finaly the Prandtl number Pr,

$$\mathrm{Re} = \frac{U_* L_*}{\nu}\,, \qquad \mathrm{Ro} = \frac{U_*}{\Omega L_*}\,, \qquad \mathrm{Fr} = \frac{U_*^2}{L_* g_*} = \frac{U_*^2}{4\pi L_*^2 G \rho_*}\,, \qquad \text{(1.32a,b,c)}$$

$$\mathcal{X} = \frac{\rho_* g_* L_*}{P_*} = \frac{\alpha_{s*}\rho_* 4\pi L_*^2 G}{T_*}\,, \qquad \mathrm{Pr} = \frac{\nu \rho_* c_p}{k} = \frac{\nu}{\kappa}\,. \qquad \text{(1.32d,e)}$$

The equation of mass conservation remains unchanged, whereas the momentum and energy equation can be rewritten (note that ρ is now dimensionless) as

$$\rho \mathrm{D}_t \mathbf{u} + \frac{2}{\mathrm{Ro}}\,\rho\,\mathbf{k}\times\mathbf{u} = -\frac{1}{\mathcal{X}\mathrm{Fr}}\,\boldsymbol{\nabla} P + \frac{1}{\mathrm{Fr}}\,\rho \mathbf{e_g} + \frac{2}{\mathrm{Re}}\boldsymbol{\nabla}\cdot(\rho \mathbf{s})\,, \qquad (1.33)$$

where $\mathbf{k}$ denotes the unit vector along the rotation axis, $\Omega\mathbf{k} = \mathbf{\Omega}$.

To simplify the following development, we have dropped here the forcing term $\mathcal{F}$. The magnetic field being maintained by convective motions, the Lorentz force will be re-introduced later in the resulting equations. This simplification although convenient, is not necessary. For a full treatment, including the Lorentz force, the reader is refered to Lantz and Fan (1999).

Finaly the entropy equation becomes

$$\rho\, T\, \mathrm{D}_t S = \frac{c_p}{\mathrm{PrRe}}\Delta T - \frac{2\mathcal{X}\mathrm{Fr}}{\alpha_{S*}\,\mathrm{Re}}\,\rho\,\mathbf{s}:\boldsymbol{\varepsilon}\,. \qquad (1.34)$$

Let us stress again, that although we use the same symbols as previously, all quantities are now dimensionless. Besides, we used the notation ":" for the double contraction of two tensors, i.e.

$$\mathbf{s}:\boldsymbol{\varepsilon} = Tr(\mathbf{s}\cdot\boldsymbol{\varepsilon}) = \mathbf{s}_{ij}\,\boldsymbol{\varepsilon}_{ji}\,. \qquad (1.35)$$

Heat transfer will be particularly important for stars and planets since it will induce convective motion directly related to dynamo action. Since we are dealing with convection, it is helpful to define a reference state. The best reference state is the neutrally stable one, of constant S (this is not the diffusive state). The governing equations can then be rewritten for deviations over this reference state. This leads to the "anelastic approximation".

It will be assumed that deviations are small compared to the reference state. This assumption is well justified in a strongly convective state and away from boundary layers.

The reference state is assumed to be fully decoupled from possible nonlinear correlations of the perturbed state, so that the dynamics of ρ_a, $\mathbf{u}_a$ and S_a is given assuming an isentropic equilibrium ($\boldsymbol{\nabla} S_a = \mathbf{0}$). Finaly, let us remind that in the limit of no thermal or radiative conduction, entropy S_a is uniform, and the corresponding temperature profile is the adiabatic profile T_a.

All quantities are expanded as

$$\rho = \rho_0 + \varepsilon_\rho \rho_1 \,, \qquad P = P_0 + \varepsilon_P P_1 \,, \tag{1.36a,b}$$

$$T = T_0 + \varepsilon_T T_1 \,, \qquad S = S_0 + \varepsilon_S S_1 \,. \tag{1.36c,d}$$

Linearization of the equation of state around the reference state provides

$$\varepsilon_\rho = \varepsilon_P = \varepsilon_T = \varepsilon_S = \varepsilon \,.$$

Let us insist that all quantities in this expansion $(\rho_0, \rho_1, P_0, P_1, T_0, T_1, S_0, S_1)$ are order one.

Mass conservation thus becomes

$$\partial_t(\rho_0 + \varepsilon\rho_1) + \boldsymbol{\nabla} \cdot [(\rho_0 + \varepsilon\rho_1)\mathbf{u}_1] = 0 \,. \tag{1.37}$$

At leading order (because ρ_0 is not a function of time)

$$\boldsymbol{\nabla} \cdot (\rho_0 \mathbf{u}) = 0 \,. \tag{1.38}$$

Neglecting higher order terms ensures the filtering of elastic waves out of the resulting model, thus the name "anelastic".

The conservation of momentum can be expressed in a similar manner

$$\begin{aligned}(\rho_0 + \varepsilon\rho_1)\left[\partial_t \mathbf{u} + (\mathbf{u}\cdot\boldsymbol{\nabla})\mathbf{u}\right] + \frac{1}{\mathcal{X}\mathrm{Fr}}\boldsymbol{\nabla}(P_0 + \varepsilon P_1) + \frac{2}{\mathrm{Ro}}(\rho_0 + \varepsilon\rho_1)\,\mathbf{k}\times\mathbf{u} \\ = \frac{1}{\mathrm{Fr}}(\rho_0 + \varepsilon\rho_1)\boldsymbol{\nabla}(\Phi_0 + \varepsilon\Phi_1) - \frac{2}{\mathrm{Re}}\boldsymbol{\nabla}\cdot\left[(\rho_0 + \varepsilon\rho_1)(\mathbf{s}_1 + \varepsilon^{1/2}\mathbf{s}_0)\right] \,.\end{aligned} \tag{1.39}$$

The coupling between energy and Navier-Stokes equations in this limiting process, necessary for convection to occur, requires $\varepsilon \sim Fr$. This scaling reveals at leading order $(1/\varepsilon)$

$$\frac{1}{\mathcal{X}}\boldsymbol{\nabla} P_0 = -\rho_0 \boldsymbol{\nabla}\Phi_0 \,. \tag{1.40}$$

Equation (1.40), together with (1.23c), provides the balance relevant for the reference state.
At the next order (ε^0), we get

$$\rho_0 \left[\partial_t \mathbf{u} + (\mathbf{u}\cdot\boldsymbol{\nabla})\mathbf{u}\right] + \frac{1}{\mathcal{X}}\boldsymbol{\nabla} P_1 + \frac{2}{\mathrm{Ro}}\rho_0 \mathbf{k}\times\mathbf{u} = -\rho_0\boldsymbol{\nabla}\Phi_1 - \rho_1\boldsymbol{\nabla}\Phi_0 - \frac{2}{\mathrm{Re}}\boldsymbol{\nabla}\cdot(\rho_0\,\mathbf{s}_1)\,. \tag{1.41}$$

It can be useful to manipulate this expression, following Braginsky and Roberts (1995, 2003), by making use of thermodynamic relations. From (1.23c)

$$\mathbf{0} = \frac{1}{\gamma}\frac{\boldsymbol{\nabla} P_0}{P_0} - \frac{\boldsymbol{\nabla}\rho_0}{\rho_0}\,, \tag{1.42}$$

while from (1.23b) and (1.23c), we obtain

$$S_1 = \frac{c_P}{T_0}\,T_1 - \frac{c_P}{\rho_0 T_0}\,P_1\,, \qquad \text{and} \qquad \alpha_S S_1 = \frac{1}{\gamma}\frac{P_1}{P_0} - \frac{\rho_1}{\rho_0}\,. \tag{1.43a,b}$$

Hence it follows that

$$\begin{aligned}
-\frac{1}{\mathcal{X}}\boldsymbol{\nabla} P_1 - \rho_0\boldsymbol{\nabla}\Phi_1 - \rho_1\boldsymbol{\nabla}\Phi_0 &= -\rho_0\boldsymbol{\nabla}\left(\frac{P_1}{\mathcal{X}\,\rho_0} + \Phi_1\right) - \frac{P_1}{\mathcal{X}\,\rho_0}\boldsymbol{\nabla}\rho_0 + \rho_1\boldsymbol{\nabla}\Phi_0\,,\\
&= -\rho_0\boldsymbol{\nabla}\left(\frac{P_1}{\mathcal{X}\,\rho_0} + \Phi_1\right) - \frac{P_1}{\mathcal{X}\,\rho_0}\boldsymbol{\nabla}\rho_0 - \left(\frac{1}{\gamma}\frac{P_1}{P_0} - \alpha_S S_1\right)\rho_0\boldsymbol{\nabla}\Phi_0 \quad \text{from (1.43b)}\\
&= -\rho_0\boldsymbol{\nabla}\left(\frac{P_1}{\mathcal{X}\,\rho_0} + \Phi_1\right) - \rho_0\alpha_S S_1\mathbf{g}_0 \quad \text{from (1.42) and (1.40).}
\end{aligned}$$

Thus equation (1.41) can be rewritten in the more compact form

$$\partial_t\mathbf{u} + \mathbf{u}\cdot\boldsymbol{\nabla}\mathbf{u} + \frac{2}{\mathrm{Ro}}\mathbf{k}\times\mathbf{u} = -\boldsymbol{\nabla}\left(\frac{P_1}{\mathcal{X}\rho_0} + \Phi_1\right) - \alpha_S S_1\mathbf{g}_0 - \frac{2}{\rho_0\,\mathrm{Re}}\boldsymbol{\nabla}\cdot(\rho_0\,\mathbf{s}_1)\,. \tag{1.44}$$

In the more general case when more than one driving mechanism is considered (e.g. thermal and chemical in the Earth's core), it can be convenient to introduce a unique variable in the momentum equation. This can be achieved by introducing a co-density variable C (see Braginsky and Roberts, 2003), which reduces in our simpler case to $C = -\alpha_S S_1$.

The entropy equation then provides

$$(\rho_0 + \varepsilon\rho_1)(T_0 + \varepsilon T_1)\left(\partial_t(S_0 + \varepsilon S_1) + \mathbf{u}\cdot\boldsymbol{\nabla}(S_0 + \varepsilon S_1)\right) = \frac{c_p}{\mathrm{Re}\,\mathrm{Pr}}\,\Delta(T_0 + \varepsilon T_1)$$

$$-\frac{2\mathcal{X}\mathrm{Fr}}{\alpha_{S*}\,\mathrm{Re}}\left(\rho_0+\varepsilon\rho_1\right)\left(\mathbf{s}_1+\varepsilon^{1/2}\mathbf{s}_0\right):\left(\boldsymbol{\varepsilon}_1+\varepsilon^{1/2}\boldsymbol{\varepsilon}_0\right). \tag{1.45}$$

At order (ε)

$$\frac{\rho_0 T_0}{c_p}\left(\partial_t S_1+\mathbf{u}\cdot\boldsymbol{\nabla}S_1\right)=\frac{c_p}{\mathrm{Re}\,\mathrm{Pr}}\,\Delta T_1-\frac{2\mathcal{X}}{\alpha_{S*}\,\mathrm{Re}}\,\rho_0\,\mathbf{s}_1:\boldsymbol{\varepsilon}_1\,. \tag{1.46}$$

Equations (1.38), (1.44), and (1.46) constitute the anelastic system.

The system governing the slow evolution of the reference state is

$$\boldsymbol{\nabla}S_0=0\,,\qquad \rho_0\boldsymbol{\nabla}P_0=\gamma P_0\boldsymbol{\nabla}\rho_0\,, \tag{1.47a,b}$$

$$\frac{1}{\mathcal{X}}\boldsymbol{\nabla}P_0=-\rho_0\boldsymbol{\nabla}\Phi_0\,,\qquad \Delta\Phi_0=\rho_0\,. \tag{1.47c,d}$$

This yields the adiabatic temperature profile, $\boldsymbol{\nabla}T_0=-\mathcal{X}\boldsymbol{\nabla}\Phi_0$, and is completed by the equation of state relating $P_0,\ \rho_0,\ T_0$.
Convection over this reference state is then governed by

$$\frac{\partial\mathbf{u}}{\partial t}+(\mathbf{u}\cdot\boldsymbol{\nabla})\mathbf{u}+\frac{2}{\mathrm{Ro}}\mathbf{k}\times\mathbf{u}=-\boldsymbol{\nabla}\left[\frac{P_1}{\mathcal{X}\rho_0}+\Phi_1\right]-\alpha_S S_1\mathbf{g}_0-\frac{2}{\mathrm{Re}\,\rho_0}\boldsymbol{\nabla}\cdot\left(\rho_0\,\mathbf{s}_1\right), \tag{1.48a}$$

$$\boldsymbol{\nabla}\cdot(\rho_0\mathbf{u})=0\,,\qquad \frac{\rho_0 T_0}{c_p}\left(\frac{\partial S_1}{\partial t}+\mathbf{u}\cdot\boldsymbol{\nabla}S_1\right)=\frac{c_p}{\mathrm{Re}\,\mathrm{Pr}}\,\Delta T_1-\frac{2\mathcal{X}}{\alpha_{S*}\,\mathrm{Re}}\,\rho_0\,\mathbf{s}_1:\boldsymbol{\varepsilon}_1\,. \tag{1.48b,c}$$

No separate equation is needed for the quantity $\boldsymbol{\nabla}\left[P_1/\mathcal{X}\rho_0+\Phi_1\right]$ since it acts as a Lagrange multiplier to satisfy $\boldsymbol{\nabla}\cdot(\rho_0\mathbf{u}_1)=0$.

Let us stress to conclude this section that under the above discussed approximation $\Phi_\Omega << \Phi_g$, the reference state only depends on the radial coordinate. The anelastic system can then be introduced as a decomposition of each variable f into a spherically averaged reference state $\overline{f}$ and a perturbation f'

$$f(r,\theta,\phi,t)=\overline{f}(r,t)+\varepsilon\,f'(r,\theta,\phi,t)$$

(e.g. Gough 1969, Latour *et al.*, 1976). This formulation allows to introduce a slow evolution of the reference state (not necessarily compatible with the above expansion).

We only derive here these equations in their simplest form. Further important effects can be introduced, such as turbulent transport coefficients (expected to be dominant in the solar convection zone). The effects of compositional convection can also be envisaged. This is a major ingredient to the Earth's core dynamics. For a complete treatment including both thermal and compositional (and also including the effect of turbulent motions), the reader is refered to Braginsky and Roberts (1995, 2000).

THE BOUSSINESQ APPROXIMATION

When the region of fluid is thin enough (in a sense to be clarified later) a more drastic approximation can be introduced, the Boussinesq approximation. It is often used for thin layers of fluid in the laboratory. Pressure effects are then unimportant, and the adiabatic temperature profile T_0 can be assumed to be constant. This allows important simplifications in the equations.

Although this is less easily jusified for the large scale astrophysical bodies described in this book, the Boussinesq approximation provides a reasonnable approximate model for the Earth core (see Chapter 4). We will therefore describe this further simplification.

If $\mathcal{X} << \mathcal{O}(1)$, i.e. if the size of the system is small compared to the typical depth of an adiabatic gas ($P_*/\rho_* g_*$), compressibility of the fluid under its own weight can safely be neglected.

For all quantities x expanded above in $x_1 + \varepsilon x_1$ [see (1.36)a–d], we now introduce a second expansion in terms of $\mathcal{X}$,

$$x_0 = x_{00} + \mathcal{X} x_{01}\,, \qquad x_1 = x_{10} + \mathcal{X} x_{11}\,. \tag{1.49a,b}$$

System (1.47c,c) at order $\mathcal{X}^{-1}$ reveals

$$\boldsymbol{\nabla} P_{00} = \mathbf{0}\,, \tag{1.51}$$

and it follows that the temperature and density of the reference profile are constant. System (1.48) at order $\mathcal{X}^{-1}$ gives

$$\boldsymbol{\nabla} P_{10} = \mathbf{0}\,, \tag{1.52}$$

while it provides at order $\mathcal{X}^0$

$$\partial_t \mathbf{u} + (\mathbf{u}\cdot\boldsymbol{\nabla})\mathbf{u} + \frac{2}{\mathrm{Ro}}\mathbf{k}\times\mathbf{u} = -\boldsymbol{\nabla}\Pi - \alpha_S S_{10}\mathbf{g}_{00} + \frac{2}{\mathrm{Re}\,\rho_0}\Delta\mathbf{u}\,, \tag{1.53a}$$

$$\boldsymbol{\nabla}\cdot\mathbf{u} = 0\,, \qquad \frac{\rho_{00}T_{00}}{c_p}\left(\frac{\partial S_{10}}{\partial t} + \mathbf{u}\cdot\boldsymbol{\nabla}S_{10}\right) = \frac{1}{\mathrm{Re}\,\mathrm{Pr}}\,\Delta T_{10}\,. \tag{1.53b,c}$$

All gradient terms have conveniently been written as $\boldsymbol{\nabla}\Pi$ in (1.53a), this term being a Lagrange multiplier to satisfy (1.53b). It follows from (1.52) that

$$S_{10} = c_P \frac{T_{10}}{T_{00}}\,. \tag{1.54}$$

We will further need to assume at this stage that we are dealing with a perfect gas, c_P can then be regarded as constant.

It is usual in the Boussinesq formalism to introduce the coefficient of "thermal expansion" α. It is defined, using dimensional variables, by

$$\frac{\delta\rho}{\rho} = \alpha\,\delta T\,, \tag{1.55}$$

and relates to the previously introduced α_S and α_P through

$$\alpha = -\frac{1}{\rho}\left(\frac{\partial\rho}{\partial T}\right)\Big|_P = \frac{\alpha_S c_P}{T_*} = \frac{\alpha_P}{T_*}\,. \tag{1.56}$$

In dimensionless from (for clarity, we introduce here a different symbol) it yields

$$\alpha' = \alpha_S c_P = \alpha_P\,. \tag{1.57}$$

System (1.48) then becomes,

$$\partial_t\mathbf{u} + (\mathbf{u}\cdot\boldsymbol{\nabla})\mathbf{u} + \frac{2}{\mathrm{Ro}}\mathbf{k}\times\mathbf{u} = -\boldsymbol{\nabla}\Pi - \alpha' T_{10}\mathbf{g}_0 + \frac{1}{\mathrm{Re}}\Delta\mathbf{u}\,, \tag{1.58a}$$

$$\boldsymbol{\nabla}\cdot\mathbf{u} = 0\,, \qquad \partial_t T_{10} + \mathbf{u}\cdot\boldsymbol{\nabla}T_{10} = \frac{1}{\mathrm{Re}\,\mathrm{Pr}}\,\Delta T_{10}\,. \tag{1.58b,c}$$

In the Boussinesq approximation the entropy and the temperature are equivalent up to a scaling factor (1.54). To recover a more classical dimensionless formalism, let us assume that a super adiabatic entropy gradient is maintained accross the system. This gradient provides the natural unit for temperature, while the velocity scale U_* can be set to κ/L_0.
One can then introduce the Rayleigh number, and the Ekman number, respectively

$$\mathrm{Ra} = \frac{\alpha\,\Delta T\,g_*\,L_*^3}{\nu\kappa}\,, \qquad \text{and} \qquad \mathrm{E} = \frac{\nu}{\Omega L_*^2}\,. \tag{1.59a,b}$$

Using (1.36), one recovers the classical system

$$\partial_t\mathbf{u} + (\mathbf{u}\cdot\boldsymbol{\nabla})\mathbf{u} + \frac{2\,\mathrm{Pr}}{\mathrm{E}}\mathbf{k}\times\mathbf{u} = -\boldsymbol{\nabla}\Pi - \mathrm{Ra}\,\mathrm{Pr}\,T\mathbf{g}_0 + \mathrm{Pr}\,\Delta\mathbf{u}\,, \tag{1.60a}$$

$$\boldsymbol{\nabla}\cdot\mathbf{u} = 0\,, \qquad \partial_t T + \mathbf{u}\cdot\boldsymbol{\nabla}T = \Delta T\,. \tag{1.60b,c}$$

Finally, it is often useful to decompose the temperature field in two contributions, a steady contribution satisfying the boundary conditions (and balancing an internal source term, if any), and a perturbation with homogeneous boundary conditions (and governed by a homogeneous equation): $T = T_s + \Theta$. Provided $\boldsymbol{\nabla}T_s\times\boldsymbol{\nabla}\Phi = 0$ (as will be the case under for a perfectly spherical problem), the resulting system is

$$\partial_t\mathbf{u} + (\mathbf{u}\cdot\boldsymbol{\nabla})\mathbf{u} + \frac{2\,\mathrm{Pr}}{\mathrm{E}}\mathbf{k}\times\mathbf{u} = -\boldsymbol{\nabla}\Pi - \mathrm{Ra}\,\mathrm{Pr}\,\Theta\mathbf{g}_0 + \mathrm{Pr}\Delta\mathbf{u}\,, \tag{1.61a}$$

$$\boldsymbol{\nabla}\cdot\mathbf{u}=0\,,\qquad \partial_t\Theta+\mathbf{u}\cdot\boldsymbol{\nabla}T_s+\mathbf{u}\cdot\boldsymbol{\nabla}\Theta=\Delta\Theta\,. \tag{1.61b,c}$$

To conclude, let us stress that since all gradient terms are included in the $\boldsymbol{\nabla}\Pi$ term (acting as a Lagrange multiplier to satisfy incompressibility), when the magnetic field is included and the Lorentz force applies, the magnetic pressure term will therefore not enter the dynamical balance. This term can produce buoyant effects in regions of localized intense field. Such magnetic buoyancy is believed to be of particular importance for solar dynamics. It is possible to construct approximations which retain this dynamical effect while considering simple incompressible fluids. This is done very much in the same way as thermal buoyancy has been retained here. We refer the reader to Spiegel & Weiss for such a derivation, achieved at the cost of relaxing (1.1c).

1.1.4. BOUNDARY CONDITIONS

When investigating a planet, a star, or a galaxy, it is convenient to consider a bounded finite volume of space $\mathcal{D}$ in which the relevant physics will be investigated. While the fluid can often be assumed to remain within this volume, the magnetic field on the other hand cannot easily be artificially confined. The first, and most natural assumption is to assume that the outside world (i.e. the complementary domain to the finite volume of interest ${}^c\mathcal{D}$) consists of vacuum and is insulating. No electrical current can therefore escape the volume $\mathcal{D}$, and the resulting $\boldsymbol{\nabla}\times\mathbf{B}=\mathbf{0}$ in ${}^c\mathcal{D}$, together with $\boldsymbol{\nabla}\cdot\mathbf{B}=0$ imply that the field in ${}^c\mathcal{D}$ derives from a potential

$$\mathbf{B}=-\boldsymbol{\nabla}\Phi\,,\qquad\text{and}\qquad \Delta\Phi=0\,. \tag{1.62a,b}$$

The above relation on the field in the complementary domain provides the necessary conditions to compute the field evolution in $\mathcal{D}$ once continuous quantities across $\partial\mathcal{D}$ are identified. Equation (1.1c) implies that $\mathbf{n}\cdot\mathbf{B}$ is continuous across the boundary, while equation (1.1a) implies the continuity of $\mathbf{n}\times\mathbf{E}$ ($\mathbf{n}$ is the normal to the boundary). These can be used to reduce the induction problem to a closed integro-differential formulation on $\mathcal{D}$ (e.g. Iskakov & Dormy, 2005).

Let us note that, while this choice of boundary condition is a very natural one and will in fact be the only one used in this book, some astrophysical bodies (like the Sun) are bounded by a conducting corona. For such corona, nothing can balance the Lorentz force in the momentum equation. As a result, the field has to relax to a state for which the Lorentz force vanishes. Such state is known as a "force-free" state. Interestingly, the field is then prescribed from the momentum equation rather than the induction equation. From $(\boldsymbol{\nabla}\times\mathbf{B})\times\mathbf{B}=\mathbf{0}$, one deduces that

$$\boldsymbol{\nabla}\times\mathbf{B}=\alpha\,\mathbf{B}\,,\qquad\text{with}\qquad (\mathbf{B}\cdot\boldsymbol{\nabla})\,\alpha=0\,, \tag{1.63a,b}$$

where α is real, and must not be confused with the notation α in meanfield theory (although the α in meanfield theory relates $\boldsymbol{\nabla} \times \mathbf{B}$ to $\mathbf{B}$ as well, it derives from a different physical reasonning). Unless α is artificially assumed to be uniform in ${}^c\mathcal{D}$, the resulting problem is non-linear and very difficult to address (even determining the necessary conditions on $\partial\mathcal{D}$ to determine $\mathbf{B}$ in ${}^c\mathcal{D}$ is not a trivial issue. So far, to the authors knowledge, no dynamo model has been produced with this type of bounding domain (even in the linear approximation). Solar models presently rely on the matching to a potential field as expressed by (1.62) (see Chapter 6).

Boundary conditions on thermodynamic quantities are, depending on the problem of the Dirichlet type (fixed value) or of the Neuman type (fixed flux).

Boundary conditions on the fluid flow usually require non-penetration of the fluid at the boundary

$$\mathbf{n} \cdot \mathbf{u} = 0\,. \tag{1.64}$$

While this condition is sufficient when viscosity is omitted, additional conditions are needed if it is retained. These usually resume for the configurations investigated in this book to either "no-slip" (1.65a) or "stress-free" (1.65b) conditions:

$$\mathbf{n} \times \mathbf{u} = \mathbf{0}\,, \qquad \text{or} \qquad \mathbf{n} \cdot \boldsymbol{\nabla}\left(\mathbf{n} \times \mathbf{u}\right) = \mathbf{0}\,. \tag{1.65a,b}$$

1.2. HOMOGENEOUS DYNAMOS

1.2.1. DISK DYNAMO

Let us now introduce the dynamo instability on an apparently very simple device: the "homopolar dynamo" or "disk dynamo". Let us consider a conducting disk of radius r, free to rotate on its axis [see Figure 1.1(a)]. If one places a permanent magnet under the disk and rotate the disk at angular velocity Ω then an electromotive force will be driven between the axis and the rim of the disk. If a conducting wire connects the rim of the disk to the axis then an electrical current will be driven through this wire. This setup was originally introduced by Faraday in 1831, it is a dynamo (it converts kinetic energy to magnetic energy), but it is not a "self-excited dynamo", since it relies on a permanent magnet. Introducing the magnetic flux through the disk $\Phi = B\pi r^2$, we can quantify this electromotive force $\mathcal{E}$ by integrating $\mathbf{u} \times \mathbf{B}$ across the disk. Assuming for simplicity a uniform and vertical field $\mathbf{B} = B\mathbf{e}_z$ one gets

$$\mathcal{E} = \frac{\Omega B r^2}{2} = \frac{\Phi\Omega}{2\pi}\,. \tag{1.66a}$$

If one now replaces the permanent magnet with a solenoid of inductance L (see Figure 1.1(b)), one faces an instability problem. If the rotation rate is small enough,

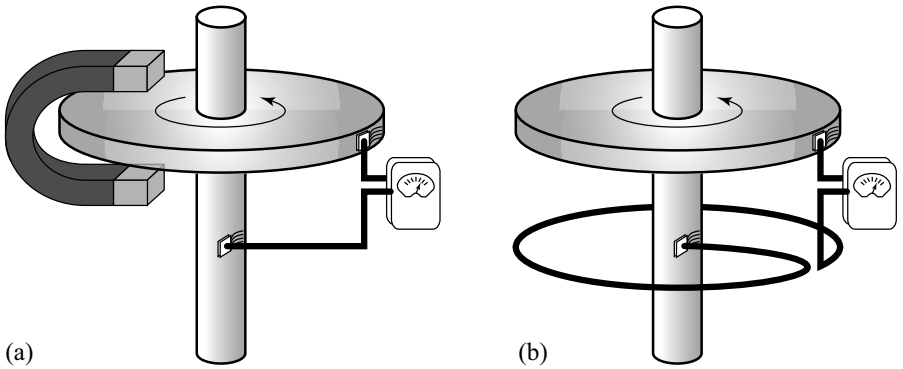

Figure 1.1 - (a) The original Faraday disk dynamo. (b) The homopolar self excited dynamo.

the resistivity will damp any initial magnetic perturbation. If the rotation rate is sufficient (in a way we will immediately quantify), then the system undergoes a "bifurcation" and an initial perturbation of field can be amplified exponentially by "self-excited dynamo action".

Let us introduce M the mutual inductance between the solenoid and the disk, which allows us, using $\Phi = MI$ to rewrite

$$\mathcal{E} = \frac{M\Omega I}{2\pi} \,. \tag{1.66b}$$

Then, R being the electrical resistivity of the complete circuit, the governing equation for the electrical currents in the system is

$$L\,\frac{dI}{dt} + R\,I = \frac{M\Omega I}{2\pi} \,. \tag{1.67}$$

It follows that the system is unstable provided

$$\Omega > \Omega_c = \frac{2\pi R}{M} \,. \tag{1.68}$$

In practice, the value of Ω_c for an experimental setup would be too high to be realistically achieved. While this setup offers a simple description of a self-excited dynamo, it cannot be constructed as such in practice (e.g. Rädler & Reinhardt, 2002).

It is worth stressing here that this mathematical description of the physical setup is oversimplified. Further developments and refinements will be dicussed later in the book. Further more, we only consider here a linear problem. The currents here appears to grow indefinitely. This is because the Lorentz force acting on the disk to

slow it down has been neglected. This force is the essence of a third setup that can also be constructed using such a disk configuration: the Barlow wheel. In this setup, no torque is externally applied to the disk. Instead a battery replaces the current-meter of Figure 1.1(a), and the interaction between this current and the externaly applied magnetic field causes the disk to rotate.

1.2.2. CHIRALITY AND GEOMETRY

The simple disk dynamo just described, of course does not possess all the features found in fluid dynamos. One property that it does possess is that of **chirality**; there is no symmetry between the system and its reflexion. The direction of rotation of the disc compared with the way in which the coil is wound (i.e. the sign of ΩM), is of crucial importance. It will be seen that chirality is very important for the production of large scale magnetic fields by fluid dynamos, though it is not essential for the production of local small scale fields; this is accomplished by stretching instead. The disc dynamo has no stretching properties, which on the face of things would suggest that magnetic energy could not be increased. However the disc dynamo is not a fluid, and current is constrained to flow in the wires and through the disc. This corresponds to a highly anisotropic electrical conductivity, while in a homogeneous fluid dynamo one expects the conductivity to be isotropic, at least to a first approximation. The key to a successful dynamo is to get the currents to flow in such a way that the resulting fields reinforce those previously existing - not a trivial task for homogeneous fluid bodies! In general currents will wish to take the shortest paths and unless the flow fields are sufficiently complicated they will simply not be able to produce the correct topology for sustained growth.

In fact it is notable that astrophysical bodies such as the Earth and Sun in which large scale fields are generated *do* in fact possess symmetry under reflection and exchange by rotation of North and South poles. So while local properties of motion in these bodies are chiral, the net lack of chirality distinguishes them from the disc problem.

1.2.3. BASIC MECHANISMS OF DYNAMO ACTION

The dynamo process is in essence a way of turning mechanical energy into magnetic energy. To see this we can take the scalar product of the induction equation (1.14) with **B**, integrate over some suitable domain and obtain, after some integration by parts and ignoring all boundary terms:

$$\frac{1}{2}\frac{\mathrm{d}}{\mathrm{d}t}\int |\mathbf{B}|^2 \mathrm{d}\mathbf{x} = \int \mathbf{B}\cdot(\mathbf{B}\cdot\boldsymbol{\nabla}\mathbf{u})\mathrm{d}\mathbf{x} - \eta\int |\boldsymbol{\nabla}\mathbf{B}|^2 \mathrm{d}\mathbf{x}\,, \tag{1.69}$$

The second term here is negative and represents the conversion of energy into heat due to Ohmic losses. The first term (due to induction) can be rewritten (in the case $\boldsymbol{\nabla}\cdot\mathbf{u}=0$) as $-\int\mathbf{u}\cdot[(\mathbf{B}\cdot\boldsymbol{\nabla})\mathbf{B}]\,\mathrm{d}\mathbf{x}$ and this is just the negative of the work done by the velocity field against the Lorentz force. Clearly there can be no growth of magnetic energy, let alone total magnetic flux, unless the induction term is effective. We can see how induction can act to increase magnetic energy by ignoring the effects of diffusion entirely. We are left with the reduced system

$$\partial_t\mathbf{B}=\boldsymbol{\nabla}\times(\mathbf{u}\times\mathbf{B})\,. \tag{1.70}$$

This is formally identical to the vorticity equation for $\boldsymbol{\omega}=\boldsymbol{\nabla}\times\mathbf{u}$ in an inviscid fluid, and we can therefore take over many results about the kinematics of vorticity (but not, note, of the dynamic aspects, since in MHD we do not have $\mathbf{B}=\boldsymbol{\nabla}\times\mathbf{u}$!). In particular, Faraday's law that the total flux threading a material element is conserved, is completely equivalent to Kelvin's circulation theorem, i.e. $\oint_{\mathcal{C}}\mathbf{u}\cdot\mathrm{d}\mathbf{x}=\int_{\mathcal{S}}\boldsymbol{\omega}\cdot\mathrm{d}\mathbf{S}$ is constant for material curves $\mathcal{C}$ spanned by material surfaces $\mathcal{S}$. This has the corollary that "vortex lines move with the fluid" (Kelvin). For magnetic fields the analogous "freezing-in" result is called Alfvén's Theorem. Consider then vortex stretching. In an extensional flow involving contraction in two directions and expansion in the third, a material tube of vortex lines aligned with the expanding direction has constant total vorticity at every cross section. Since the cross sectional area is diminishing, the local vorticity must increase, and so since the volume is fixed the integral of $|\boldsymbol{\omega}|^2$ also increases. Exactly the same argument can be applied to magnetic fields, with the result that such stretching flows can increase magnetic energy. Note, however that the total magnetic flux is not increased, so this mechanism as it stands is not able to account for any increases in e.g. dipole moments in conducting spheres. In addition, in a finite domain stretching must be accompanied by folding, as in kneading dough, and this second action will in general bring oppositely directed fields together, where they will cancel due to Ohmic dissipation. This does not always happen though, as can be seen from the Vainshtein-Zeldovich dynamo (the *Stretch-Twist-Fold, or STF mechanism*) leads to the effective doubling of the energy of a loop of flux, as shown in Figure 1.2. This is the most dramatic example of a number of transformations of the space that can lead to net stretching. More explicit examples of the consequences of folding and stretching are given in Section 1.6. There are outstanding questions as to whether such folding can exist throughout a homogeneous fluid; in general some cancellation will occur. In particular, when fields and flows are two–dimensional there is always too much folding, cancellation always dominates stretching and fields will decay. A simple example is provided by the non-dimensional flow field $\mathbf{u}=(-x,0,z)$ (where the timescale has been based on a typical velocity U_0 and a typical length $\mathcal{L}$), with $\mathbf{B}=(0,0,B(x,t))$. From (1.14) we can see, introducing $\mathrm{Rm}=U_0\mathcal{L}/\eta$, that B obeys

$$\partial_t B-x\,\partial_x B=B+\mathrm{Rm}^{-1}\,\partial_{xx}B\,. \tag{1.71}$$

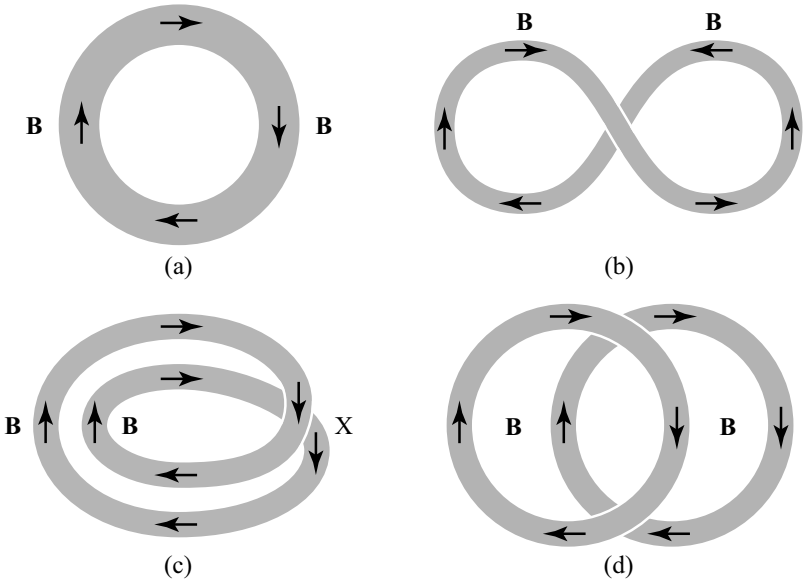

Figure 1.2 - Sketch of the STF mechanism (after Fearn *et al.*1988). The final magnetic flux is doubled.

If $B(x,0) = \mathrm{Re}\left\{\beta_0\, \mathrm{e}^{\mathrm{i}k_0 x}\right\}$ then

$$B(x,t) = \mathrm{Re}\left\{\beta_0\, \exp\left[t - k_0^2(\mathrm{e}^{2t}-1)/2\mathrm{Rm}\right]\, \exp\left(\mathrm{i}k_0\, \mathrm{e}^t x\right)\right\}\,, \tag{1.72}$$

so that $|B|$ eventually decays superexponentially. This is due to diffusion acting on the exponentially increasing gradients caused by folding. In spite of this, however, we can have transient growth of magnetic energy for long times $\sim \ln(\mathrm{Rm}/k_0^2)$. As $\mathrm{Rm} \to \infty$ energy can increase indefinitely. This example is instructive in that it points up the singular nature of the infinite Rm limit; the limits of large times and large conductivity cannot be interchanged.

1.2.4. FAST AND SLOW DYNAMOS

An important application of dynamo theory is to astrophysical applications, in which we need to understand the behaviour of dynamo growth rates when $\mathrm{Rm}$is very large. When Rm is of order unity, the two intrinsic timescales, associated with the turnover time and the Ohmic diffusion rate are comparable, but at large Rm the turnover/advective timescale is much shorter, while the Ohmic time is longer than any recognisable magnetic process. Thus we ask; can magnetic energy (or magnetic flux or dipole moment) grow at a rate independent of η as $\eta \to 0$? This leads to the distinction between fast and slow dynamos. The subject is treated in much greater

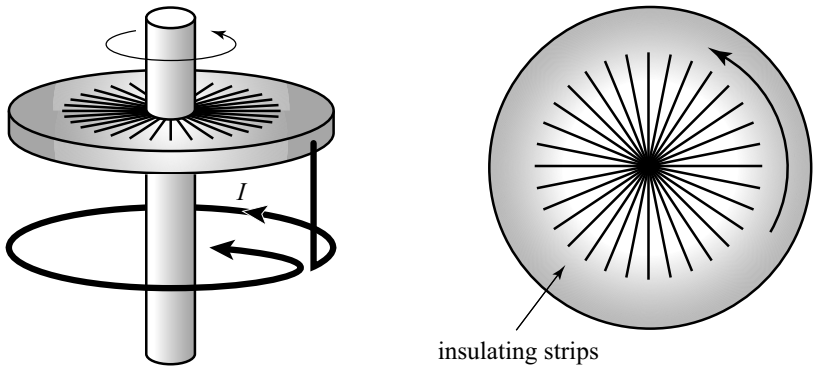

Figure 1.3 - The segmented Faraday dynamo (Moffatt, 1979). The insulating strips in the inner part of the disc ensure that the current is radial there.

detail in Section 1.6: here we give only a brief outline, concentrating on the problem of growth of flux at large Rm.

For a *slow dynamo* growthrates (on the advective timescale) $\rightarrow 0$ as $\mathrm{Rm} \rightarrow \infty$, while for a *fast dynamo* growthrates (or at least the $\limsup$ if there are many modes) do not tend to zero at large Rm. In this case the field appears on all scales as $\mathrm{Rm} \rightarrow \infty$, and diffusion can never be neglected. This important point was first made by Moffatt and Proctor (1985). While as we have seen it is easy to produce an increase in magnetic energy if diffusion is entirely neglected, an increase of magnetic *flux* of dipole moment can only occur due to the presence of diffusion (as shown by Faraday's Law). This is necessary to get round flux conservation as diffusion becomes negligible. The Faraday disc dynamo has been discussed in Section 1.2.1. Here we examine a modification introduced by Moffatt (1979), which illustrates the *rôle* of diffusion in preventing fast dynamo action. This is the segmented Faraday dynamo (see also the brief discussion in Section 2.8). It is best understood by reference to Figure 1.3; the difference from the usual single disc dynamo geometry, as shown in Figure 1.3 is that currents are constrained to move radially on the disc except near the outer edge.

We can write down simple equations relating current in the wire I, current round the disc J, the angular velocity Ω and the fluxes through the wire and disc, respectively, Φ_I, Φ_J. We obtain

$$\Phi_I = LI + MJ, \quad \Phi_J = MI + L'J, \quad RI = \Omega\Phi_J - \frac{\mathrm{d}\Phi_I}{\mathrm{d}t}, \quad R'J = -\frac{\mathrm{d}\Phi_J}{\mathrm{d}t}\,. \tag{1.73}$$

We seek solutions $\propto \mathrm{e}^{pt}$. As for the usual dynamo, we find growth if $\Omega M > R$. The

growthrate is

$$p_+ = \frac{\sqrt{(RL' + R'L)^2 + 4R'(\Omega M - R)(LL' - M^2)} - (RL' + R'L)}{2(LL' - M^2)}\,. \quad (1.74)$$

We can see that $p_+ > 0$ for all $\Omega > R/M$ but $p_+ \sim \sqrt{\Omega R'}$ as $\Omega \to \infty$. Thus the growthrate is controlled by diffusion and not exclusively by advection, and in particular the growthrate tends to zero on the advective timescale Ω^{-1}.

We shall discuss further aspects of fast and slow dynamo action in realistic flows in Section 1.3; the whole subject of the fast dynamo problem is treated in much more detail in Section 1.6.

1.3. NECESSARY CONDITIONS FOR DYNAMO ACTION

1.3.1. DEFINITIONS OF DYNAMO ACTION

In this section, we describe various rigorous results concerning dynamo action. It is helpful first to give a precise definition of what is meant by dynamo action: the definition depends on the geometry considered. We can consider either a bounded conductor surrounded by insulator, or magnetic fields and flows defined in a periodic box. Many generalizations are possible (for example, one could consider the effects of an external stationary conductor, as was done by Proctor, 1977a), but the details complicate the analysis.

Case 1: *Finite conductor.*
Suppose $\mathbf{B}$ is defined in a finite volume $\mathcal{D}$, surrounded (in ${}^c\mathcal{D}$) by an insulator. In ${}^c\mathcal{D}$ we have $\boldsymbol{\nabla} \times \mathbf{B} = \mathbf{0}$, with all components of $\mathbf{B}$ continuous at $\partial\mathcal{D}$, because there are no surface currents. We suppose no currents at infinity, so that $|\mathbf{B}| \sim \mathcal{O}(|\mathbf{x}|^{-3})$ as $|\mathbf{x}| \to \infty$.

Case 2: *Periodic dynamo.*
$\mathbf{B}$ is defined in a periodic domain $\mathcal{D} \in \mathbb{R}^3$, with $\int_{\mathcal{D}} \mathbf{B}\, d\mathbf{x} = \mathbf{0}$.

In each case $\mathbf{u}$ satisfies $\boldsymbol{\nabla}\cdot\mathbf{u} = 0$, and has time-bounded norm (for Case 2, we choose a frame so that the mean value of $\mathbf{u}$ vanishes. Several different norms can be defined, for example $\mathsf{U} \equiv \max_{\mathcal{D}}(|\mathbf{u}|)$, $\mathsf{S} \equiv \max_{\mathcal{D},i,j}(|\partial_j u_i|)$, $\mathsf{E}^{1/2} \equiv \left(\int_{\mathcal{D}} |\boldsymbol{\nabla}\mathbf{u}|^2 d\mathbf{x}\right)^{1/2}, \ldots$, etc. In Case 1, we suppose that $\mathbf{u} = \mathbf{0}$ on $\partial\mathcal{D}$ (this is not strictly necessary for some of the bounds but aids the analysis). Then we can define the magnetic energy $\mathcal{M} = \frac{1}{2}\int |\mathbf{B}|^2\, \mathrm{d}\mathbf{x}$ where the integral is over $\mathbb{R}^3$ in Case 1, or over $\mathcal{D}$ in Case 2. The usual requirement for dynamo action is that $\mathcal{M}$ does not tend to zero as $t \to \infty$.

1.3.2. NON-NORMALITY OF THE INDUCTION EQUATION

In the next subsections we give several criteria which, if violated, rule out dynamo action. These are *necessary conditions*. It is notable that there are no general sufficient conditions known for dynamo action; working dynamos can only be found by explicit integration of particular flows. This is because the induction equation, considered as a parabolic linear operator, is *non-normal*; when $\mathbf{u}$ is independent of time, the eigenvectors found by looking for solutions $\propto \exp(pt)$ are not orthogonal, and so even when all eigenvectors p have negative real part, i.e. when we have a non-dynamo, the magnetic energy can still increase for some time. The condition that the energy decays is much stronger than that the spectrum is in the left hand half plane. The situation is analogous to that of the stability of shear flows, for which the energy stability result of Orr gives a bound on the Reynolds number that is far below observed stability thresholds. A simple example of this effect is provided by the interaction of a purely zonal flow with a meridional field in a sphere. For large Rm the zonal field increases more rapidly than the meridional field decays, leading to transient growth of the magnetic energy, but the meridional field eventually decays and the whole system runs down.

1.3.3. FLOW VELOCITY BOUNDS

If we nonetheless try to find conditions for the decay of the magnetic energy, we focus on (1.69), which gives us in Case 1

$$\frac{\mathrm{d}\mathcal{M}}{\mathrm{d}t} = \mathcal{P} - \eta\mathcal{J}\,, \tag{1.75}$$

where $\mathcal{P}$ and $\mathcal{J}$ can take the alternative forms:

$$\mathcal{P} = \int_{\mathcal{D}} \mathbf{B}\cdot(\mathbf{B}\cdot\boldsymbol{\nabla}\mathbf{u})\,\mathrm{d}\mathbf{x} = \int_{\mathcal{D}} (\mathbf{u}\times\mathbf{B})\cdot(\boldsymbol{\nabla}\times\mathbf{B})\,\mathrm{d}\mathbf{x}\,, \tag{1.76}$$

$$\mathcal{J} = \int_{\mathcal{D}} |\boldsymbol{\nabla}\times\mathbf{B}|^2\,\mathrm{d}\mathbf{x} = \int_{\mathbb{R}^3} |\boldsymbol{\nabla}\mathbf{B}|^2\,\mathrm{d}\mathbf{x}\,, \tag{1.77}$$

(for Case 2, we have the same results, but all integrals are taken over $\mathcal{D}$).

In order to construct the proofs we shall need a *Poincaré inequality*. Defining $\mathcal{F} = \frac{1}{2}\mathcal{J}/\mathcal{M}$, we have $\mathcal{F} \geq c^{-2}$; $c \propto (\int_{\mathcal{D}} \mathrm{d}\mathbf{x})^{1/3}$. For a sphere of radius a, $c = a/\pi$, while for a periodic cube of side a, $c = a/2\pi$. The proof of this result can either be done by the standard methods of variational calculus, or by expressing the magnetic field in terms of spherical harmonics.

Using the above inequality together with (1.75) in the case that $\mathcal{P} = 0$ (stationary conductor) we have the result that $\mathrm{d}(\ln\mathcal{M})/\mathrm{d}t \leq -2\,\eta\,c^{-2}$, so that the magnetic

energy decays exponentially at a finite rate. It is not surprising, then that a finite velocity is needed for dynamo action to be possible. We can find bounds on each of the three norms defined above. We have the following bounds on $\mathcal{P}$:

$$\begin{aligned}
&\text{(a)} \quad \mathcal{P} \le \mathsf{U}\int_{\mathcal{D}} |\mathbf{B}\cdot\boldsymbol{\nabla}\mathbf{B}|d\mathbf{x} \le \mathsf{U}(2\mathcal{M})^{1/2}\mathcal{J}^{1/2} \quad \text{Childress (1969)}\,,\\
&\text{(b)} \quad \mathcal{P} \le \mathsf{S}(2\mathcal{M}) \quad \text{Backus (1958)}\,,\\
&\text{(c)} \quad \mathcal{P} \le \mathsf{E}^{1/2}\left(\int_{\mathcal{D}} |\mathbf{B}|^4 d\mathbf{x}\right)^{1/2} \le \mathsf{E}^{1/2}c_1(2\mathcal{M})^{1/4}\mathcal{J}^{3/4} \quad \text{Proctor (1979)}\,,
\end{aligned}$$

where c_1 is a dimensionless constant (Proctor (1979) gives the value 4). Using these results we can get three bounds on the exponential growthrate $\sigma = \mathrm{d}(\ln\mathcal{M})/\mathrm{d}t$:

$$\begin{aligned}
&\text{(a)} \quad \frac{1}{2}\sigma \le \mathcal{F}^{1/2}(\mathsf{U} - \eta c^{-1})\,,\\
&\text{(b)} \quad \frac{1}{2}\sigma \le \mathsf{S} - \eta c^{-2}\,,\\
&\text{(c)} \quad \frac{1}{2}\sigma \le \mathcal{F}^{3/4}(c_1\mathsf{E}^{1/2} - \eta c^{-1/2})\,.
\end{aligned}$$

So if $\mathcal{M}$ is not to tend to zero we must have $\mathsf{U} > \eta/c$, $\mathsf{S} > \eta/c^2$, $\mathsf{E} > \eta^2/cc_1^2$. (The first result can be proved under the less restrictive assumption $\mathbf{u}\cdot\mathbf{n} = 0$ on $\partial\mathcal{D}$.) Because $\mathcal{F}$ has a minimum value we can get upper bounds on σ in cases (a) and (c) that do not involve $\mathcal{F}$:

$$\begin{aligned}
&\text{(a)} \quad \frac{1}{2}\sigma \le \max\left[(\mathsf{U}/c - \eta c^{-2}), \frac{\mathsf{U}^2}{4\eta}\right]\,,\\
&\text{(c)} \quad \frac{1}{2}\sigma \le \max\left[(c_1\mathsf{E}^{1/2}c^{-3/2} - \eta c^{-2}), \frac{27c_1^4\mathsf{E}^2}{256\eta^3}\right]\,.
\end{aligned}$$

It is notable that none of these bounds involves the kinetic *energy* $\mathcal{K} = \frac{1}{2}\int_{\mathcal{D}} |\mathbf{u}|^2 d\mathbf{x}$ of the velocity field. In fact a working dynamo can be found with arbitrarily small energy. Consider a velocity field $\mathbf{u}$ in a sphere of radius R surrounded by stationary conductor. For a steady dynamo the induction equation is invariant under $\mathbf{x} \to \mathbf{x}/R$, $\mathbf{u} \to R\mathbf{u}$, $\mathcal{K} \to R\mathcal{K}$. Thus as $R \to 0$ the necessary energy $\to 0$. The argument can be extended to the case where the conductor is replaced outside some large radius by an external insulator.

1.3.4. GEOMETRICAL CONSTRAINTS

These conditions are of two kinds; restrictions on the nature of *flows* that can give growing field, and constraints on the types of *field* that can be sustained by dynamo action. In the first category, until recently the best result was the *toroidal theorem* of Elsasser (1946), Bullard & Gellman (1954) (see also Moffatt, 1978). For Case 1, if we multiply (1.14) by $\mathbf{r} \equiv r\,\mathbf{e}_r$ and integrate then we obtain (defining $P = \mathbf{B}\cdot\mathbf{r}$, $Q = \mathbf{u}\cdot\mathbf{r}$),

$$\partial_t P + \mathbf{u}\cdot\boldsymbol{\nabla} P = \mathbf{B}\cdot\boldsymbol{\nabla} Q + \eta\Delta P \ \text{ in } \mathcal{D}\,, \tag{1.78}$$

with $\Delta P = 0$ in ${}^c\mathcal{D}$, and $P, \partial P/\partial r$ continuous on $\partial\mathcal{D}$.

If $\boldsymbol{\nabla}\cdot\mathbf{u} = 0$, we can separate $\mathbf{u}$ into toroidal and poloidal parts $\mathbf{u}_T$, $\mathbf{u}_P$, where

$$\mathbf{u} = \mathbf{u}_T + \mathbf{u}_P \equiv \boldsymbol{\nabla}\times(\phi\,\mathbf{r}) + \boldsymbol{\nabla}\times\boldsymbol{\nabla}\times(\psi\,\mathbf{r})\,. \tag{1.79}$$

It follows that $Q = L_2\psi$, where L_2 is the angular momentum operator, defined as

$$L_2 = (\mathbf{r}\cdot\boldsymbol{\nabla})^2 - r^2\Delta\,. \tag{1.80}$$

A similar decomposition can be made for $\mathbf{B}$, with

$$\mathbf{B}_T = \boldsymbol{\nabla}\times(T\,\mathbf{r})\,,\ \mathbf{B}_P = \boldsymbol{\nabla}\times\boldsymbol{\nabla}\times(S\,\mathbf{r})\,,\ \text{with } P = L_2 S\,. \tag{1.81a,b,c}$$

If therefore the velocity field is toroidal, $\psi = 0$ and so Q also vanishes. Then (1.78) reduces to a sourceless diffusion-type equation for P, so that

$$\tfrac{1}{2}\partial_t \int_{\mathcal{D}} P^2 \mathrm{d}\mathbf{x} = -\eta \int_{\mathbb{R}^3} |\boldsymbol{\nabla} P|^2 \mathrm{d}\mathbf{x} < -\eta c^{-2} \int_{\mathcal{D}} P^2 \mathrm{d}\mathbf{x} \ \Rightarrow |P| \to 0\,. \tag{1.82}$$

Once $|P|$ and so $|\mathbf{B}_P|$ becomes negligible the equation for the toroidal part of the induction equation can also be simplified. Now $\mathbf{u}$, $\mathbf{B}$ are both toroidal, and

$$\boldsymbol{\nabla}\times(\mathbf{u}\times\mathbf{B}_T) = \boldsymbol{\nabla}\times[-\mathbf{r}(\mathbf{u}\cdot\boldsymbol{\nabla} T)]\,. \tag{1.83}$$

After "uncurling" (integrating and setting the arbitrary function of r that arises to zero without loss of generality), we obtain

$$\partial_t T + \mathbf{u}\cdot\boldsymbol{\nabla} T = \eta\Delta T\,, \text{with } T = 0 \ \text{ on } \ \partial\mathcal{D}\,. \tag{1.84}$$

Apart from the boundary conditions this is the same equation as satisfied by P, and we can show by similar means that $\int_{\mathcal{D}} T^2 d\mathbf{x} \to 0$ (exponentially) also. While this result does not rule out a transient increase in the magnetic energy of $\mathbf{B}_T$, which depends upon mean square gradients of T, it can be shown that if the magnetic energy does *not* tend to zero then $\mathcal{F}$ must increase without bound, and so eventually

Childress' result above will be violated, giving a contradiction. Thus a dynamo is impossible.

A similar result holds in cartesian coordinates (Case 2), when $\mathbf{u}\cdot\mathbf{z}=0$, then

$$\partial_t B_z + \mathbf{u}\cdot\boldsymbol{\nabla}B_z = \mathbf{B}\cdot\boldsymbol{\nabla}u_z + \eta\Delta B_z\,, \tag{1.85}$$

and we can apply exactly analogous reasoning (Zeldovich, 1957).

Busse (1975) used (1.78) when $Q\neq 0$ to obtain a bound on the ratio of toroidal and poloidal field energies. We have

$$\begin{aligned}\frac{1}{2}\frac{\mathrm{d}}{\mathrm{d}t}\int_{\mathcal{D}} P^2\mathrm{d}\mathbf{x} &= -\int_{\mathcal{D}} Q\mathbf{B}\cdot\boldsymbol{\nabla}P\mathrm{d}\mathbf{x} - \eta\int_{\mathbb{R}^3}|\boldsymbol{\nabla}P|^2\mathrm{d}\mathbf{x}\\ &\leq \max_{\mathcal{D}} Q\left(2\mathcal{M}\cdot 2\int_{\mathbb{R}^3}|\mathbf{B}_P|^2\,\mathrm{d}\mathbf{x}\right)^{1/2} - 2\eta\int_{\mathbb{R}^3}|\mathbf{B}_P|^2\,\mathrm{d}\mathbf{x}\end{aligned}$$

where the inequality $\int_{\mathbb{R}^3}|\mathbf{B}_P|^2\mathrm{d}\mathbf{x}\leq\frac{1}{2}\int_{\mathbb{R}^3}|\boldsymbol{\nabla}P|^2\mathrm{d}\mathbf{x}$ has been used (see, for example, Proctor, 2004). Then we have the result that

$$\max_{\mathcal{D}} Q \geq \eta\left(\frac{1}{\mathcal{M}}\int_{\mathbb{R}^3}|\mathbf{B}_P|^2\,d\mathbf{x}\right)^{1/2}. \tag{1.86}$$

Though this result may be useful in interpreting geomagnetic data, it is not of course an anti-dynamo theorem. Nonetheless it turns out that (as might be expected) dynamo action can be ruled out if the poloidal flow is sufficiently weak for any given toroidal flow. In fact it is possible to find inequalities for time derivatives of P^2 and T^2, namely (choosing some constant $\mu>0$)

$$\frac{1}{2}\frac{\mathrm{d}}{\mathrm{d}t}\left(\int_{\mathcal{D}}(P^2+\mu T^2)\mathrm{d}\mathbf{x}\right)\leq\left(\frac{aU_P}{\sqrt{2}}-\eta\right)(\mathcal{P}^2+\mu\mathcal{T}^2)+\left[a^2U_P+\frac{\mu}{2}(U_T+U_P)\right]\mathcal{P}\mathcal{T}\,, \tag{1.87}$$

where $\mathcal{P}^2=\int_{\mathbb{R}^3}|\boldsymbol{\nabla}P|^2\mathrm{d}\mathbf{x}$, $\mathcal{T}^2=\int_{\mathcal{D}}|\boldsymbol{\nabla}T|^2\mathrm{d}\mathbf{x}$, and U_P, U_T are the maxima of $|\mathbf{u}_P|$, $|\mathbf{u}_T|$ respectively in $\mathcal{D}$. For an appropriate choice of μ we can show that the best possible condition under which the left hand side is negative definite is

$$a^2U_P\,(U_T+U_P)-2\left(\eta-\frac{aU_P}{\sqrt{2}}\right)^2<0 \quad\text{or}\quad a^2U_PU_T+2\sqrt{2}\eta aU_P<2\eta^2 \tag{1.88a,b}$$

(Proctor, 2004). Poincaré inequalities may be used to show that the integrals of both P^2 and T^2 decay exponentially, and this implies eventual decay of the magnetic energy as argued above. The result (1.88a,b) does not rule out dynamo action when the velocity field $\mathbf{u}$ is purely poloidal; and indeed there are examples in the literature

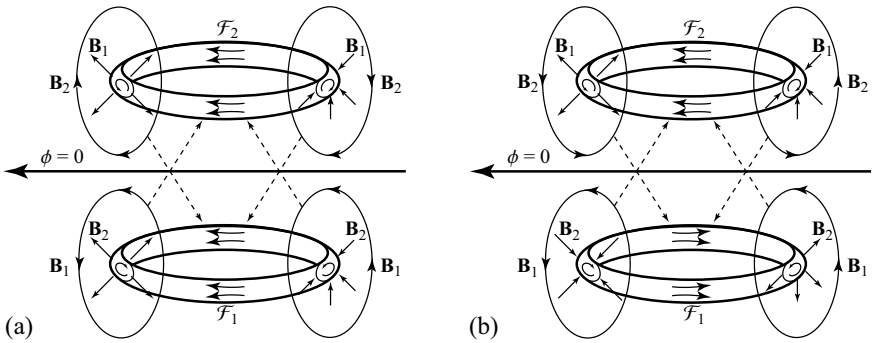

Figure 1.4 - The poloidal dynamo of Gailitis (from Gailitis 1970). The flow is axisymmetric, while the magnetic field is proportional to $\mathrm{e}^{\mathrm{i}\phi}$. Two different parities of solution are shown. Suffix 1 refers to fields generated by the lower ring, suffix 2 those due to the upper ring. For more details see e.g. Fearn *et al.*(1988)

of dynamos with purely poloidal velocity fields. A classic example is provided by the twin-torus dynamo of Gailitis (Gailitis, 1970), see Figure 1.4.

As regards constraints on the field, the main result is *Cowling's Theorem* (Cowling, 1934): An axisymmetric magnetic field cannot be maintained by dynamo action. It should be noted that if $\mathbf{B}$ is axisymmetric then so is $\mathbf{u}$ but the converse is not true, and the dynamo of Gailitis (1970) above provides an example of an axisymmetric flow field which acts as a dynamo for non-axisymmetric fields. There are several proofs of this in various cases. We first follow the proof of Braginsky (1964). We again assume $\boldsymbol{\nabla} \cdot \mathbf{u} = 0$, and that the conducting region $\mathcal{D}$ is spherical. Since $\mathbf{B}, \mathbf{u}$ are axisymmetric we can separate the zonal and meridional parts of (1.14) by writing (in polar coordinates (s, ϕ, z));

$$\mathbf{B} = B\mathbf{e}_\phi + \boldsymbol{\nabla} \times (A\mathbf{e}_\phi) = B\,\mathbf{e}_\phi + \mathbf{B}_P\,, \qquad \mathbf{u} = \mathbf{u}_P + U\,\mathbf{e}_\phi\,. \tag{1.89a,b}$$

Since there are no imposed zonal currents, we get

$$\partial_t A + \frac{1}{s}\mathbf{u}_P \cdot \boldsymbol{\nabla}(sA) = \frac{1}{\mathrm{Rm}}\left(\Delta - \frac{1}{s^2}\right) A\,, \tag{1.90a}$$

$$\partial_t B + s\mathbf{u}_P \cdot \boldsymbol{\nabla}\left(\frac{B}{s}\right) = s\mathbf{B}_P \cdot \boldsymbol{\nabla}\left(\frac{U}{s}\right) + \frac{1}{\mathrm{Rm}}\left(\Delta - \frac{1}{s^2}\right) B\,. \tag{1.90b}$$

Further simplification ensues if we write $A = \chi/s$, $B = \psi s$, $U = \Omega s$. Then we obtain the alternative system

$$\frac{\partial \chi}{\partial t} + \mathbf{u}_P \cdot \boldsymbol{\nabla}\chi = \eta\left(\Delta - \frac{2}{s}\frac{\partial}{\partial s}\right)\chi\,, \tag{1.91a}$$

$$\frac{\partial \psi}{\partial t} + \mathbf{u}_P \cdot \boldsymbol{\nabla}\psi = \mathbf{B}_P \cdot \boldsymbol{\nabla}\Omega + \eta\left(\Delta + \frac{2}{s}\frac{\partial}{\partial s}\right)\psi\,, \tag{1.91b}$$

with $(\Delta - (2/s)\partial/\partial s)\chi = \psi = 0$ in ${}^c\mathcal{D}$ and $\chi \sim \mathcal{O}(|\mathbf{x}|^{-1})$ as $|\mathbf{x}| \to \infty$. It is notable that the toroidal field does not appear in the equation for χ. The analysis now proceeds in a similar manner to that for the toroidal theorem. We form the poloidal "energy equation"

$$\frac{1}{2}\frac{\mathrm{d}}{\mathrm{d}t}\int_{\mathcal{D}}\chi^2\mathrm{d}\mathbf{x} = \eta\int_{\mathcal{D}}\chi\left(\Delta - \frac{2}{s}\frac{\partial}{\partial s}\right)\chi\mathrm{d}\mathbf{x} = -\eta\int_{\mathbb{R}^3}|\boldsymbol{\nabla}\chi|^2\mathrm{d}\mathbf{x} \le -\eta\, c_3^2\int_{\mathcal{D}}\chi^2\mathrm{d}\mathbf{x}\,. \tag{1.92}$$

It is then clear that $\chi^2 \to 0$, and so by arguments used in the previous subsection, eventually the poloidal field will decay also. When χ is negligible, we can form a similar relation for ψ and show similarly that

$$\begin{aligned}\frac{1}{2}\frac{\mathrm{d}}{\mathrm{d}t}\int_{\mathcal{D}}\psi^2\mathrm{d}\mathbf{x} &= \eta\int_{\mathcal{D}}\psi\left(\Delta + \frac{2}{s}\frac{\partial}{\partial s}\right)\psi\,\mathrm{d}\mathbf{x}\\ &= -\eta\left(\int_{\mathcal{D}}|\boldsymbol{\nabla}\psi|^2\mathrm{d}\mathbf{x} + 2\pi\int_{-a}^{a}\psi(0,z)^2\,\mathrm{d}z\right)\,,\end{aligned} \tag{1.93}$$

and so $\psi^2 \to 0$ also. We can prove very similar results for fields (and so flows) that are independent of z.

There are other types of proofs of Cowling's theorem, which allow us to generalise the problem to permit η to depend on position. They show the impossibility of the maintenance of a steady magnetic field against Ohmic decay when there is a neutral curve on which the meridional field vanishes at an O-type neutral point. Suppose that this is at $\mathbf{X}$, and consider a small meridional circle S_ε centred at $\mathbf{X}$, boundary C_ε, radius ε, with $B_\varepsilon \equiv (2\pi\varepsilon)^{-1}\oint_{C_\varepsilon}|\mathbf{B}_P|\mathrm{d}\mathbf{x}$,

$$(\max_{\mathcal{D}}|\mathbf{u}|)B_\varepsilon S_\varepsilon \ge \int_{S_\varepsilon}(\mathbf{u}_P\times\mathbf{B}_P)\cdot\mathrm{d}\mathbf{x} = \int_{S_\varepsilon}\eta(\mathbf{x})\boldsymbol{\nabla}\times\mathbf{B}_P\cdot\mathrm{d}\mathbf{x} \sim 2\pi\varepsilon B_\varepsilon\eta(\mathbf{X})\,. \tag{1.94}$$

This leads to a contradiction as $S_\varepsilon \sim \varepsilon^2$. The neutral ring argument, while in some sense more general than the Braginsky proof in that the field does not have to be exactly axisymmetric, is more limited in other ways, since the result of the proof is to rule out steady fields (for steady flows) and so has nothing to say about exponential decay. Fuller details are given in Moffatt (1978) and Fearn *et al.* (1988).

When the flow is not incompressible useful results are harder to find. The equation for χ is still correct. Since $\chi(0,z) = 0$ and $\chi \to 0$ as $|\mathbf{x}| \to \infty$, there must exist a positive maximum of χ, at $\mathbf{X}(t)$ where $\boldsymbol{\nabla}\chi = \mathbf{0}$, $\Delta\chi \le 0$. This rules out a growing dynamo with a poloidal field. Hide & Palmer (1982) have argued that if $\Delta\chi(\mathbf{X}) = 0$ for all time then χ becomes non-differentiable near $\mathbf{X}$ and so $\mathbf{B}_0 \to \mathbf{0}$. The arguments used are appealing but are hard to rigorize. They have been criticized by Ivers & James (1984). These authors have used maximum principles to show that both poloidal and toroidal fields decay exponentially, but the bounds for the decay

rates so far found are not useful, in that the associated decay times are much longer than that of any astrophysical body. The question of how far a properly selected compressible flow in a sphere can reduce the Ohmic decay rate for an axisymmetric field remains partially open.

1.4. STEADY AND TIME-DEPENDENT VELOCITIES

In this short section, we discuss the differences between the dynamo properties of steady and time-dependent flow fields. This is necessary because so much of our intuition on the efficacy of dynamo action is based on thinking about steady flows, and these can be misleading in the general case.

1.4.1. TWO SIMPLE EXAMPLES

Smooth, steady flows $\mathbf{u}$ are not usually efficient as dynamos at large Rm, because there is not enough stretching. In particular, smooth axisymmetric or 2D flows cannot be fast dynamos if they are steady, since there is then no exponential stretching of material lines (the relation between stretching properties of the flow and growth rates at large Rm has been discussed earlier, and will be treated in much more detail in the following). On the other hand time-dependent flows can be very efficient as dynamos, even if they have a very simple Eulerian form. As an example consider two related flows, the so-called [G.O.] Roberts (Roberts, 1970) and Galloway–Proctor (GP) (Galloway & Proctor, 1992) flows

$$\begin{aligned} \text{Roberts flow:}\quad \mathbf{u}(x,y) &\propto \boldsymbol{\nabla}\times(\psi(x,y)\,\mathbf{e}_z)+\gamma\psi(x,y)\,\mathbf{e}_z\,, \\ \psi &= \sin x\sin y\,; \end{aligned} \tag{1.95}$$

$$\begin{aligned} \text{GP-flow:}\quad \mathbf{u}(x,y,t) &\propto \boldsymbol{\nabla}\times(\psi(x,y,t)\,\mathbf{e}_z)+\gamma\psi(x,y,t)\,\mathbf{e}_z\,, \\ \psi &= \sin(y+\varepsilon\sin\omega t)+\cos(x+\varepsilon\cos\omega t)\,. \end{aligned} \tag{1.96}$$

The Roberts flow has three components, but depends only on x and y. It has a fixed cellular pattern; there is no stretching except at the cell corners. The GP-flow has a very similar cellular structure in the Eulerian flow, but the cellular pattern rotates. The consequences for the stretching properties are profound; there is stretching (positive Liapunov exponent) almost everywhere (see Figure 1.5). We can find dynamo action for both these flows by looking for fields of the form $\mathbf{B} = \mathrm{Re}\left\{\widetilde{\mathbf{B}}(x,y,t)\mathrm{e}^{\mathrm{i}\,k\,x}\right\}$. Then the growthrate (for the GP-flow the average growthrate over one time period of the flow) depends on Rm and k.

(a) 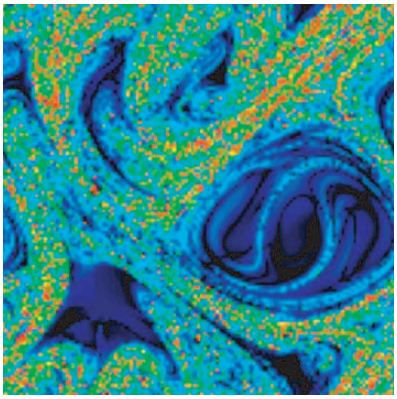 (b) 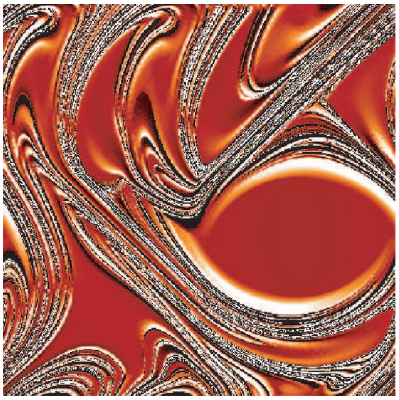

Figure 1.5 - Chaos in the GP-flow. (a) finite-time Liapunov exponents (after Cattaneo *et al.* 1996) for $\omega = 1$, $\varepsilon = 1$, showing there is exponential stretching almost everywhere. (b) normal field B_z (courtesy of F. Cattaneo). Note the large regions of multiply folded field. (**See color insert**.)

For the Roberts flow the optimum growthrate occurs at large wavenumber[2] k for $\mathrm{Rm} \gg 1$, and in fact $k \sim (\mathrm{Rm}^{1/2}/\ln \mathrm{Rm})$. As $\mathrm{Rm} \to \infty$ the optimum growthrate is $\sim \mathcal{O}(\ln(\ln \mathrm{Rm})/\ln \mathrm{Rm})$, see Figure 1.6. So this flow is not (quite) a fast dynamo.

The GP-flow is completely different. The growthrate is $\mathcal{O}(1)$ for large Rm, and the optimum wavenumber also $\mathcal{O}(1)$. Here the flow is chaotic, and though there are thin flux structures, chaotic regions near the stagnation points do not scale with Rm. The choice of k for optimum growth is presumably related to the widths of these structures. Time dependent flows of this type have proved a fertile ground for extensive numerical simulation of fast dynamo properties.

1.4.2. PULSED FLOWS

Another important aspect of time-dependent flows is that many restrictions that would prevent dynamo action for the instantaneous flow field do not apply when the flow is time dependent. This is associated with the non-normality of the induction equation, as discussed above. As a particular example we show how the Toroidal and Zeldovich theorems can be got round for time-dependent flows. Consider the

2 The scale k^{-1}, though small compared to the cell size, is long compared to the thin boundary layer scale $\mathrm{Rm}^{-1/2}$ for field near stagnation points.

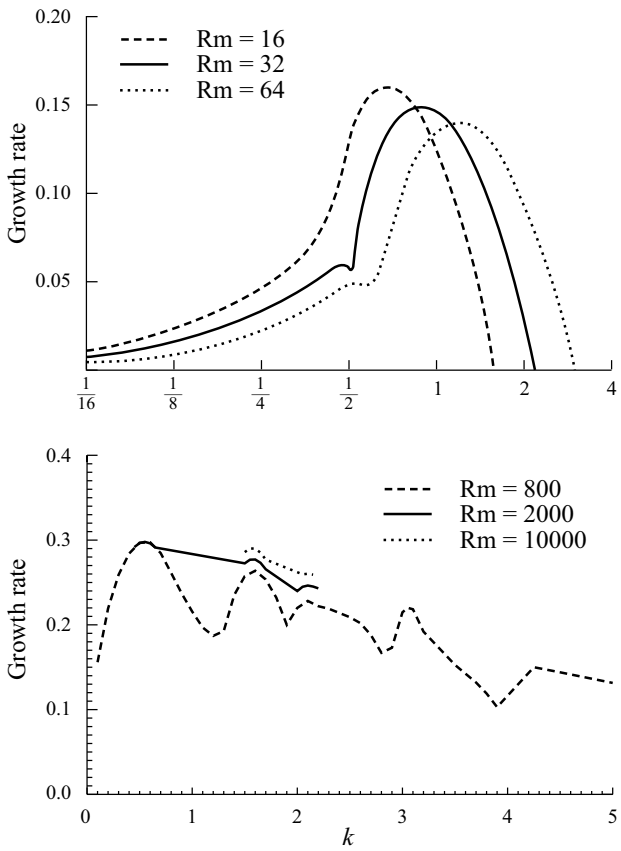

Figure 1.6 - Growth rates for the Roberts and GP flows, as functions of Rm and k. Top figure shows the Roberts flow, with peak growthrates decreasing at large Rm, and the critical k increasing. Bottom figure shows the same data for the GP flow with $\varepsilon = \omega = 1$. Note the convergence of the growthrate and critical wavenumber for large Rm.

pulsed Beltrami flow (Soward, 1993).

$$\mathbf{u} = \begin{cases} (0, \sin x, \cos x) & (0 \le t \le \tau) \\ (\sin y, 0, \cos y) & (\tau \le t \le 2\tau), \ \text{ etc.} \end{cases} \tag{1.97}$$

This is a planar flow at all but isolated discrete times, but during each interval τ we can have transient growth, and this can lead to dynamo action. The development is most easily seen when we set $\eta = 0$ (for small η the results are almost the same as long as τ is not too large). In the interval $(0 \le t \le \tau)$ consider the horizontally averaged field $\overline{\mathbf{B}} \equiv \mathrm{Re}\left\{\widetilde{\mathbf{B}}_H \exp(\mathrm{i}kz)\right\}$, then

$$\overline{\mathbf{B}}_H(\tau) = J_0(k\tau)\overline{\mathbf{B}}_H(0) - \mathrm{i}\tau J_1(k\tau)\overline{B_x}(0)\,\mathbf{e}_y\,, \tag{1.98}$$

which can be large for large τ. If we add (small) diffusion, we still get growth, provided τ is much less than the diffusion time. Then the second pulse can refold and stretch the field and give further enhancement. A more complicated version of this kind of flow is one that arises in thermal convection, where there is a homoclinic connection between two different planar flows. In this case the flow is not a dynamo, because the interval between switching of the flows tends to infinity. The addition of noise to the system, however, will render the switching time finite and can induce instability. For further details see Gog *et al.*(1999).

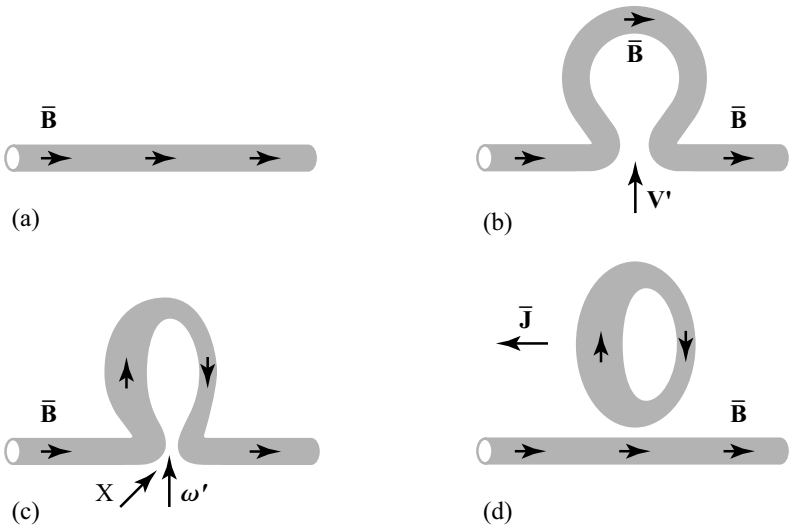

Figure 1.7 - The cyclonic event mechanism as envisaged by Parker (after Roberts, 1994). The uniform field in (a) is pulled up in (b), twisted in (c), and then reconnects to form a field loop with a normal component (and so EMF) anti-parallel to the original field (d).

1.5. TWO–SCALE DYNAMOS

1.5.1. THE TWO–SCALE CONCEPT AND PARKER'S MODEL

The dynamo flows we have already met: Roberts, GP and pulsed flows and extensions to 3D flows such as the ABC model (see section 1.6, and Childress & Gilbert 1995) are small scale dynamos. The magnetic field has scales comparable to that of $\mathbf{u}$. But if $\mathbf{B}$ exists on two distinct scales then dynamo action can be easily verified. Perhaps the simplest model is that of Parker (1955). Suppose that small scale "cyclonic events" act on a uniform field. If the velocity of these small-scale motions has non-zero *helicity*, i.e. $\mathbf{u} \cdot \boldsymbol{\nabla} \times \mathbf{u} \neq 0$, then the field is twisted by the motion as in Figure 1.7. By Ampère's Law (1.3) there is generated an EMF parallel to the original field. The sign of this EMF is opposite to the helicity for short-lived events. However for longer lived events there is not in general any such clear correlation. If these helical motions are distributed isotropically then any EMF perpendicular to the field will cancel out when an average is taken over all events. When this new EMF is incorporated, we get an extra term $\boldsymbol{\nabla} \times \alpha \mathbf{B}$ on the rhs of (1.14); this new term is called the α–effect. An extended discussion including nonlinear effects is given in Section 2.7 and Chapter 6.

Parker's model of the solar magnetic field supposes that the large scale field is ax-

isymmetric. The crucial *rôle* of the α–effect is to sustain poloidal from toroidal field. The same mechanism is also capable of sustaining toroidal from poloidal field, but is ignored in his model in favour of the much more effective *rôle* of zonal shears. We then obtain the model system

$$\partial_t A + \frac{1}{s}\,\mathbf{u}_P \cdot \boldsymbol{\nabla}(sA) = \alpha B + \frac{1}{\mathrm{Rm}}\left(\Delta - \frac{1}{s^2}\right) A\,, \tag{1.99a}$$

$$\partial_t B + s\,\mathbf{u}_P \cdot \boldsymbol{\nabla}\left(\frac{B}{s}\right) = [\boldsymbol{\nabla} \times (\alpha \boldsymbol{\nabla} \times \mathbf{B}_P)] + s\,\mathbf{B}_P \cdot \boldsymbol{\nabla}\left(\frac{U}{s}\right) + \frac{1}{\mathrm{Rm}}\left(\Delta - \frac{1}{s^2}\right) B\,. \tag{1.99b}$$

We discuss solutions of this equation below when we have looked at a more systematic derivation.

1.5.2. MEAN FIELD ELECTRODYNAMICS

We now suppose formally that the magnetic and velocity fields exist on a small scale ℓ and a large scale L, and/or on short and long time scales. We may then define some average over the short scales (denoted by $\overline{\cdots}$) and write $\mathbf{B} = \overline{\mathbf{B}} + \mathbf{B}'$, $\mathbf{u} = \overline{\mathbf{u}} + \mathbf{u}'$, etc. Then, taking the average,

$$\partial_t \overline{\mathbf{B}} = \boldsymbol{\nabla} \times \boldsymbol{\mathcal{E}} + \boldsymbol{\nabla} \times (\overline{\mathbf{u}} \times \overline{\mathbf{B}}) - \boldsymbol{\nabla} \times (\eta \boldsymbol{\nabla} \times \overline{\mathbf{B}})\,, \tag{1.100}$$

where $\boldsymbol{\mathcal{E}} \equiv \overline{\mathbf{u}' \times \mathbf{B}'}$.

In order to calculate $\boldsymbol{\mathcal{E}}$ we need to find $\mathbf{B}'$, whose equation is

$$\partial_t \mathbf{B}' = \boldsymbol{\nabla} \times (\overline{\mathbf{u}} \times \mathbf{B}') + \boldsymbol{\nabla} \times (\mathbf{u}' \times \overline{\mathbf{B}}) \tag{1.101}$$

$$+ \boldsymbol{\nabla} \times (\mathbf{u}' \times \mathbf{B}' - \overline{\mathbf{u}' \times \mathbf{B}'}) - \boldsymbol{\nabla} \times (\eta \boldsymbol{\nabla} \times \mathbf{B}')\,. \tag{1.102}$$

This equation can only be solved in special cases but we can make some general remarks about the nature of $\boldsymbol{\mathcal{E}}$. Clearly, for fixed $\mathbf{u}'$, $\mathbf{B}'$ depends linearly on $\overline{\mathbf{B}}$ and so $\boldsymbol{\mathcal{E}}$ is a linear functional of $\overline{\mathbf{B}}$. Assuming the simplest possible local relation, we obtain the expression

$$\mathcal{E}_i = \alpha_{ij} \overline{B}_j - \beta_{ijk}\,\partial_j \overline{B}_k + \ldots \tag{1.103}$$

α_{ij} is a pseudo-tensor; the symmetric part is non-zero only if the statistics of $\mathbf{u}$ lack mirror-symmetry. The anti-symmetric part, on the other hand, acts like a velocity and because of this it can only be non-zero if the statistics lack homogeneity, or if there is anisotropy combined with broken reflection symmetry. If we suppose that the statistics of $\mathbf{u}'$ are isotropic but not mirror-symmetric, then $\alpha_{ij} = \alpha\delta_{ij}$.

We can relate the pseudo-scalar α to the helicity of the small-scale flow. Both arise from broken mirror-symmetry, and we can give explicit relations in limiting cases.

We can similarly simplify the second term in the expansion for $\boldsymbol{\mathcal{E}}$, for in the isotropic case $\beta_{ijk} = \beta\varepsilon_{ijk}$, which can be identified as a "turbulent magnetic diffusivity".

All the foregoing assumes that $\mathbf{B}'$ owes its existence entirely to $\overline{\mathbf{B}}$. In this case, in particular, the value of α can be determined simply by making $\overline{\mathbf{B}}$ uniform, in which case $\mathcal{E}_i$ is exactly $\alpha_{ij}\overline{\mathbf{B}}_j$. However, as we have already seen, when Rm is large enough there is a possibility, indeed a likelihood that a small-scale field can exist even when $\overline{\mathbf{B}} = \mathbf{0}$. It is hard to see how to interpret the α–effect in this situation since any "mean-field" effect has to exist on top of an already equilibrated small-scale field. The problem is then intrinsically nonlinear and so beyond the scope of this section, though it will be considered in the next chapter.

Supposing that indeed $\boldsymbol{\mathcal{E}}$ owes its existence to $\overline{\mathbf{B}}$, we can see that the α–effect can lead to dynamo action. Consider (writing $\eta + \beta = \eta'$)

$$\partial_t \overline{\mathbf{B}} = \boldsymbol{\nabla} \times (\alpha \overline{\mathbf{B}}) - \boldsymbol{\nabla} \times (\eta \boldsymbol{\nabla} \times \overline{\mathbf{B}}) \,. \tag{1.104}$$

If α, β are uniform, we get solutions of form $\mathrm{Re}\left\{\widehat{\mathbf{B}} \exp(i\mathbf{k}\cdot\mathbf{x} + pt)\right\}$, with $(p + \eta' k^2)^2 = \alpha^2 k^2$, so $p_+ > 0$ for all sufficiently small k. It can thus be seen that mean-field dynamo action is inevitable on all sufficiently large scales, provided only that $\alpha \neq 0$.

The α tensor will take more general forms with lower symmetry of flow statistics. In a sphere, when there are two preferred directions, namely the rotation $\boldsymbol{\Omega}$ and the radial vector $\mathbf{r}$, we will get the more general form

$$\boldsymbol{\mathcal{E}} = \alpha_1(\boldsymbol{\Omega}\cdot\mathbf{r})\overline{\mathbf{B}} + \alpha_2 \mathbf{r}(\boldsymbol{\Omega}\cdot\overline{\mathbf{B}}) + \alpha_3 \boldsymbol{\Omega}(\mathbf{r}\cdot\overline{\mathbf{B}}) + \ldots \tag{1.105}$$

Note that both rotation and a preferred direction would seem necessary for an α–effect.

A detailed discussion of possible forms of $\boldsymbol{\mathcal{E}}$ in various cases is given by Krause & Rädler (1980).

As explained above it is hard to calculate α in the general case. There are two special cases in which analytical progress can be made:

(a) If Rm, based on the small length scale ℓ, is very small, then there is no small-scale dynamo. We calculate α by approximating the equation for $\mathbf{B}'$ by

$$0 = \overline{\mathbf{B}}\cdot\boldsymbol{\nabla}\mathbf{u}' + \eta\Delta\mathbf{B}' \,, \tag{1.106}$$

with $\overline{\mathbf{B}}$ uniform. If we consider, as an example, $\mathbf{u}'$ in the simple Fourier form $\propto \mathrm{Re}\left\{\mathrm{e}^{\mathrm{i}\mathbf{k}\cdot\mathbf{x}}\right\}$ then we have $B_i' = \mathrm{i}\overline{B}_j k_j u_i'/\eta k^2$ so

$$\mathcal{E}_i = \alpha_{ij}\,\overline{B}_j = \mathrm{i}\,\varepsilon_{ipq}\,k_j\,\overline{u_p'^* u_q'}\;\overline{B}_j/\eta k^2 \,. \tag{1.107}$$

If we choose coordinates in which $\mathbf{k} = (0, 0, k)$ then $\mathcal{E}_i = \alpha_{ij}\overline{\mathbf{B}}_j$ where $\alpha_{ij} = \alpha\delta_{i3}\delta_{j3}$ and $\alpha\eta k^2 = -\varepsilon_{ijk}k_j\overline{u_i'^* u_k'}$. The latter quantity is just the helicity, and so as predicted from Parker's ansatz we see that α has the opposite sign to the helicity. Adding together many modes of this type, we can reproduce α due to any velocity field.

(b) The "short-sudden" approximation. This is used when the small-scale Rm is *large*, and thus is harder to justify. In general the fluctuating field $\mathbf{B}'$ will be much larger than the mean field, and so extra assumptions have to be made to simplify the equations. We suppose that the fluctuating velocity field, and so the fluctuating magnetic field, becomes decorrelated on a time τ_c short enough that the correlated part of $\mathbf{B}'$ is again small compared to $\overline{\mathbf{B}}$. We ignore diffusion. Then $\partial_t\mathbf{B}' \approx \overline{\mathbf{B}}\cdot\boldsymbol{\nabla}\mathbf{u}'$. This can be solved to give $B_i' \approx \tau_c\overline{\mathbf{B}}\cdot\boldsymbol{\nabla}\mathbf{u}'$, so in the isotropic case

$$\alpha = -\frac{\tau_c}{3}\,\overline{\mathbf{u}'\cdot\boldsymbol{\nabla}\times\mathbf{u}'}\,. \tag{1.108}$$

Again we see that α is anticorrelated with helicity.

The approximations involved in both these limits essentially ignore the self-interaction of $\mathbf{u}'$ and $\mathbf{B}'$ in the $\mathbf{B}'$ equation. The equation becomes intractable when these terms are not ignored, and so apart from these extreme cases it is hard to give useful results. However there is one result available without approximation in Gruzinov & Diamond (1994). If we suppose the fields and flow statistically steady with uniform imposed field $\overline{\mathbf{B}}$ (and periodic boundary conditions for simplicity), and, using the vector potential introduced in (1.16), write $\mathbf{B}' = \boldsymbol{\nabla}\times\mathbf{A}'$, we then have

$$\partial_t\mathbf{A}' = -\boldsymbol{\nabla}\Phi + \overline{\mathbf{u}}\times\mathbf{B}' + \mathbf{u}'\times\overline{\mathbf{B}} \tag{1.109}$$

$$+\,\mathbf{u}'\times\mathbf{B}' - \overline{\mathbf{u}'\times\mathbf{B}'} - \eta\boldsymbol{\nabla}\times\mathbf{B}'\,, \tag{1.110}$$

so (ignoring boundary terms that arise from integration by parts)

$$0 = \tfrac{1}{2}\left(\overline{\mathbf{B}'\cdot\partial_t\mathbf{A}' + \mathbf{A}'\cdot\partial_t\mathbf{B}'}\right) = -\overline{\mathbf{B}}\cdot\boldsymbol{\mathcal{E}} - \eta\overline{\mathbf{B}'\cdot\boldsymbol{\nabla}\times\mathbf{B}'}\,. \tag{1.111}$$

This holds without approximation if boundary terms are ignored. Thus in the isotropic case

$$\alpha|\overline{\mathbf{B}}|^2 = -\frac{\eta}{3}\,\overline{\mathbf{B}'\cdot\boldsymbol{\nabla}\times\mathbf{B}'}\,. \tag{1.112}$$

This result gives some guidance about the behaviour of α as the small-scale Rm increases. In particular, it shows that diffusion must be included in any proper model of α. If α is independent of η at large Rm, leading to a fast mean field dynamo, and we posit that $|\mathbf{B}'| \sim \eta^a|\overline{\mathbf{B}}|$, $|\boldsymbol{\nabla}\times\mathbf{B}'| \sim \eta^{-1/2}|\mathbf{B}'|$, and is intermittent with a filling factor $\sim \eta^b$, then $2a + b = -1/2$. Possible solutions include $b = 1/2$, $a = -1/2$ giving sheet-like fields, while if the fields are primarily tubes rather than sheets we might expect $a = -1$, so $b = 3/2$.

1.5.3. MEAN FIELD MODELS

If the α–effect is accepted as a model of the effects of small-scale flows on the large scale field, then Cowling's theorem does not apply, since now toroidal field can sustain poloidal field, and so we can investigate axisymmetric models. Physical considerations (the *rôle* of the Coriolis force in inducing helicity) suggest that in a rotating body such as the Earth or the Sun α is odd about the equator. Similar considerations suggest that the zonal flow U should be even, so we can get two types of field structure: (i) Dipole: where B is odd about the equator, and A is even. (ii) Quadrupole; A is odd, B is even. Examples of fields of the two types are shown in Figure 1.9.

Most models are one of two types: (i) "α^2", with U neglected. This has been used to model stationary e.g. planetary dynamos; (ii) "$\alpha\omega$" in which the α term in (1.99b) is neglected, as in the Parker model. α^2 models typically give steady dynamos (real growthrates) while $\alpha\omega$ models usually give cyclic dynamos (complex growthrates). We can understand the latter in terms of dynamo waves. We use cartesian geometry; let

$$A = A(x,t)\,, \qquad B = B(x,t)\,, \qquad \mathbf{B}_p \cdot \boldsymbol{\nabla} U \sim \omega \partial_x A\,, \qquad \text{(1.113a,b,c)}$$

where x is a variable corresponding to latitude (the term (1.113c) is referred to as the ω–effect). Substituting into (1.99), and modelling radial derivatives with a constant damping term, we obtain the simplified system (compare to Equation (6.1a,b) in Chapter 6).

$$\partial_t A = \alpha B + \eta\left(\partial_{xx} A - K^2 A\right)\,, \quad \partial_t B = \omega\,\partial_x A + \eta\left(\partial_{xx} B - K^2 B\right)\,. \quad \text{(1.114a,b)}$$

This has travelling wave solutions with $A, B \propto \exp\left[\mathrm{i}k(x-ct)\right]$ when

$$\alpha\omega = \pm 2\eta^2 (k^2+K^2)^2/k\,, \qquad c = -\alpha\omega/[2\eta(k^2+K^2)]\,. \qquad \text{(1.115)}$$

Note that the modulus of the dynamo number $D = \alpha\omega/\eta^2 K^3$ takes a minimum value $16/3\sqrt{3}$ when $k = K/\sqrt{3}$. Note the definite sign of the wave speed c which depends on the sign of D.

In a spherical geometry $\alpha\omega$ models can be used to give models of the solar cycle (butterfly diagram) by identifying large B with regions of sunspot eruption. Forms of α, U and any meridional velocity are prescribed, and the equations solved numerically as an eigenvalue problem to obtain marginal (periodic solutions). A particularly comprehensive study was carried out by Roberts (1972). While these kinematic studies are now overshadowed by the dynamical studies reported on later, it is interesting to note that travelling waves of activity, similar to the Parker waves, can be seen propagating latitudinally. The direction of propagation depends on the sign

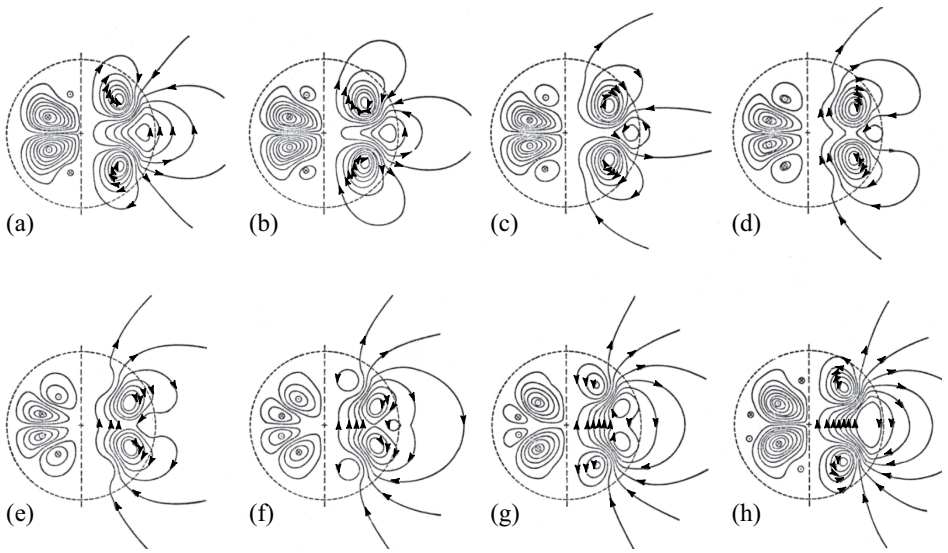

Figure 1.8 - Oscillatory Dipolar solutions for an $\alpha - \omega$ dynamo (from Roberts, 1972).

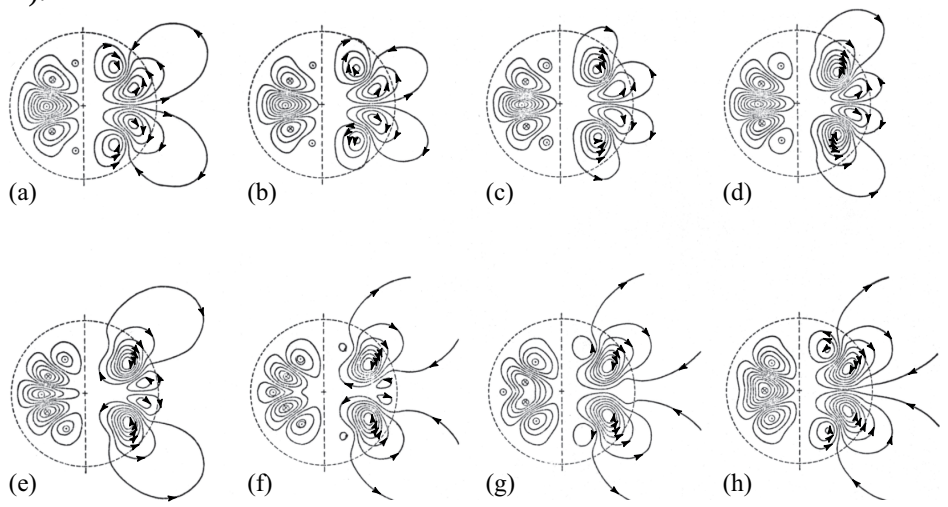

Figure 1.9 - As above, but quadrupolar solutions.

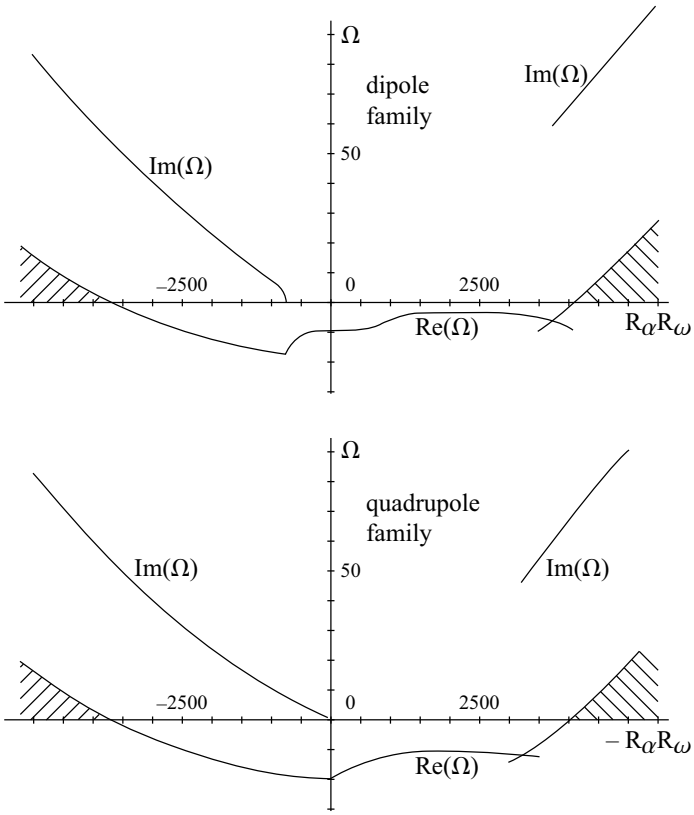

Figure 1.10 - Real and imaginary parts of the growth rate for typical α–ω dynamos (from Roberts, 1972). Unstable regions are shaded. The x–axis is reversed in the lower figure. Note the similarity between the figures, as suggested in Proctor (1977b).

of the dynamo number, and since on the Sun the waves move towards the equator we can make some deductions about the dynamics leading to α. The associated frequency of oscillation also emerges from the calculation and is comparable with the turbulent diffusion time.

There is an interesting near symmetry, associated with the adjoint dynamo problem, between dipole (quadrupole) modes with $\alpha, \mathbf{u}$, and quadrupole (dipole) modes with $\alpha, -\mathbf{u}$ (Proctor, 1977b). This is illustrated in Figure 1.10, which shows growth rates for a particular dynamo model. The figures for the different parities are very similar, though the x–axis, measuring the dynamo number is reversed in the right-hand figure.

We can relate these results to the well known butterfly diagram of the solar cycle (shown in Figure 6.3, page 290 and discussed in Section 6.1). If we identify the

sites of sunspot activity with maxima of B, (since we believe that sunspots are manifestations of large toroidal fields through the magnetic buoyancy instability), then the equatorward propagation of the disturbances will lead to a picture like the observations.

These global models of dynamo action have been superseded by models in which the shear is concentrated just below the convective zone of the sun, and so the α–effect is separated spatially from the shear. This "interface model" (Parker, 1993), which also leads to dynamo waves, will be discussed in detail along with its dynamical consequences in Chapter 6.

1.6. LARGE MAGNETIC REYNOLDS NUMBERS

Let us now turn to the evolution of magnetic fields under the induction equation at large magnetic Reynolds number, as explained in Section 1.2.4. We will begin by giving a formal definition, before discussing the motivation for such studies and presenting various examples. For further information and more references than can easily be provided here see the reviews Childress (1992), Bayly (1994), Soward (1994), Childress & Gilbert (1995) and Gilbert (2003).

Suppose we have a given incompressible flow $\mathbf{u}$ with a typical length scale $\mathcal{L}$ and velocity scale U, and the magnetic diffusivity is η. Then after non-dimensionalisation using these scales, the induction equation (1.14) becomes

$$\partial_t \mathbf{B} + \mathbf{u}\cdot\boldsymbol{\nabla}\mathbf{B} = \mathbf{B}\cdot\boldsymbol{\nabla}\mathbf{u} + \varepsilon\Delta\mathbf{B}\,, \tag{1.116a}$$

where $\varepsilon^{-1} \equiv \mathrm{Rm} = U\mathcal{L}/\eta$ is the magnetic Reynolds number, and

$$\boldsymbol{\nabla}\cdot\mathbf{B} = 0\,, \qquad \boldsymbol{\nabla}\cdot\mathbf{u} = 0\,. \tag{1.116b,c}$$

For a given flow $\mathbf{u}$ and an $\varepsilon > 0$, dynamo action may take place, the fastest growing magnetic field mode having an exponential growth rate $\gamma(\varepsilon)$; for example for a steady flow

$$\mathbf{B}(\mathbf{x},t) \propto \mathbf{b}(\mathbf{x})\mathrm{e}^{\sigma t}, \qquad \gamma = \mathrm{Re}\,\{\sigma\}\ . \tag{1.117}$$

The flow $\mathbf{u}$ is a *fast dynamo* if the *fast dynamo exponent*

$$\gamma_0 \equiv \lim_{\varepsilon\to 0}\gamma(\varepsilon) \tag{1.118}$$

is positive; otherwise it is a *slow dynamo*. For a fast dynamo, magnetic field growth occurs on the turnover time-scale of the underlying flow $\mathbf{u}$ (on which we first non-dimensionalised), independently of molecular diffusion. A slow dynamo operates on a slower, diffusion-limited time-scale, as we shall see in some examples below.

Why study fast dynamos? Before answering this question, it is best to widen the scope of our enquiry: our interest is in dynamo mechanisms (fast and slow) at large Rm, the structure of magnetic fields, and the saturation of dynamo instabilities (in which case (1.116a) must be supplemented by an equation for $\mathbf{u}$). Mathematically, the limit $\mathrm{Rm} \to \infty$ or $\varepsilon \to 0$ in (1.116a) is a singular limit as ε multiplies the highest derivative, and so this requires careful treatment by numerical codes, or by asymptotic means. Taking this limit allows a clear subdivision of dynamos and unstable magnetic modes into different families, as we shall see. This classification can be useful even if Rm is not particularly large in an application; however in many astrophysical applications Rm is very large, and dynamo processes do appear to operate on fast time-scales; for example in the Sun Rm is of the order of 10^8 and the magnetic field oscillates on the fast, 11-year Solar cycle.

Finally, developing mathematical tools to cope with fast dynamos is a considerable challenge with wider application, for example to vorticity and passive scalar transport in complex flows (e.g., Reyl, Antonsen & Ott, 1998; Fereday *et al.* 2002). The induction equation (1.116a) is challenging because the behaviours as $\varepsilon \to 0$ and for $\varepsilon = 0$ are markedly different at large times. If one simply sets $\varepsilon = 0$, then the induction equation corresponds to advecting a vector field $\mathbf{B}$ in the given flow $\mathbf{u}$, field lines being frozen in the fluid. The field will gain finer and finer scales, and the magnetic energy will grow because of field stretching. Because of this reduction of scale, there are no well-behaved eigenfunctions for a general flow in the case $\varepsilon = 0$ (Moffatt & Proctor, 1985). Now suppose diffusion is introduced: this can have very dramatic effects because of the fine scales in the field. For example for a typical planar flow $\mathbf{u}(x, y, t) = (u_1, u_2, 0)$, the magnetic energy grows indefinitely for $\varepsilon = 0$, but for any $\varepsilon > 0$ it eventually decays, in keeping with the anti-dynamo theorem for planar flows discussed in Section 1.3.4.

In this short review we will consider examples of slow and fast dynamos in flows and mappings, but only make passing reference to issues of dynamo saturation; these will be taken up in Chapter 2.

1.6.1. SLOW DYNAMOS IN FLOWS

Perhaps the simplest example of a slow dynamo is the Ponomarenko dynamo (e.g., Ponomarenko, 1973; Gilbert, 1988; Ruzmaikin, Sokoloff & Shukurov, 1988). In cylindrical polar coordinates (r, θ, z),

$$\mathbf{u} = r\Omega(r)\mathbf{e}_\theta + U(r)\mathbf{e}_z\,; \tag{1.119}$$

this is a swirling helical flow, depending only on radius r. Here we focus on the case of a smooth flow, although Ponomarenko's original paper had piecewise constant U and Ω. Related flows were studied by Lortz (1968).

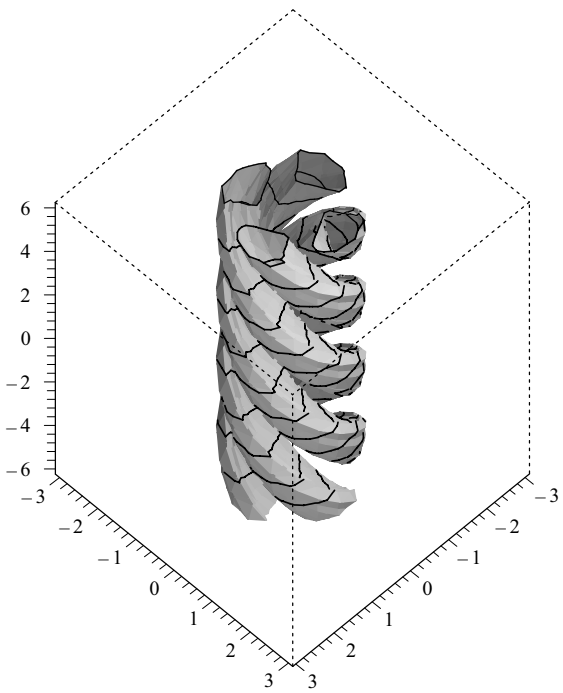

Figure 1.11 - Magnetic field in the Ponomarenko dynamo at large magnetic Reynolds number $\mathrm{Rm} = \varepsilon^{-1}$ forms spiralling tubes of field localised near the resonant stream surface.

We may consider a magnetic mode $\mathbf{B} = \mathbf{b}(r)\,\exp\left[\mathrm{i}m\theta + \mathrm{i}kz + \sigma t\right]$, classified by wavenumbers m and k. In this case the induction equation (1.116a) for b_r and b_θ becomes

$$\left[\sigma + \mathrm{i}\,m\,\Omega(r) + \mathrm{i}\,k\,U(r)\right]\,b_r = \varepsilon\,\left[(\Delta_m - r^{-2})\,b_r - 2\,\mathrm{i}\,m\,r^{-2}b_\theta\right]\,, \tag{1.120a}$$

$$\left[\sigma + \mathrm{i}\,m\,\Omega(r) + \mathrm{i}\,k\,U(r)\right]\,b_\theta = r\,\Omega'(r)\,b_r + \varepsilon\,\left[(\Delta_m - r^{-2})\,b_\theta + 2\,\mathrm{i}\,m\,r^{-2}b_r\right]\,. \tag{1.120b}$$

We can drop the b_z equation as b_z can be reconstructed from the condition $\boldsymbol{\nabla}\cdot\mathbf{B} = 0$. The basic mechanism can be seen in these two equations, and can be described as of $\alpha\omega$-type. The stretching of radial field by the gradient of angular velocity $\Omega'(r)$ generates b_θ field in equation (1.120b) (an ω–effect), while diffusion of b_θ field in curved geometry can generate radial field by the last term in (1.120a) (broadly speaking, an α–effect).

To obtain formulae for growth rates at small ε, we rescale, so as to capture the fastest growing modes, setting

$$m = \varepsilon^{-1/3}M\,,\quad k = \varepsilon^{-1/3}K\,,\quad r = a + \varepsilon^{1/3}s\,. \tag{1.121a,b,c}$$

Here we are seeking a mode localised at a radius a (whose significance we will discover shortly) in the interior of the fluid. We scale the growth rate as

$$\sigma = \varepsilon^{-1/3}\sigma_0 + \sigma_1 + \varepsilon^{1/3}\sigma_2 + \cdots\,, \tag{1.122}$$

and for the field, set

$$b_r = \varepsilon^{1/3}b_{r0}(s) + \cdots\,,\qquad b_\theta = b_{\theta0}(s) + \cdots\,, \tag{1.123a,b}$$

These expansions are then to be substituted into (1.120a,b) and the flow field (1.119) also Taylor-expanded about $r = a$ in powers of s. When this is done, corresponding powers of ε are equated, to give at the leading two orders:

$$\sigma_0 + \mathrm{i}\,M\,\Omega(a) + \mathrm{i}\,K\,U(a) = 0\,, \tag{1.124a}$$

$$\mathrm{i}\,M\,\Omega'(a) + \mathrm{i}\,K\,U'(a) = 0\,,\quad \sigma_1 = 0\,. \tag{1.124b,c}$$

The first simply fixes σ_0 as purely imaginary, advection of the magnetic field mode by the flow at radius a. The second condition implies that a mode with given (m,k) tends to localise at the radius a where the shear of the flow is aligned with field lines, assuming such a radius exists; if it does not, then we may expect the mode to localise at a boundary.

At the next order we obtain from (1.120) coupled parabolic cylinder equations, which may be written in the form

$$(c_0 + \mathrm{i}\,c_2\,s^2 - \partial_s^2)\,b_{r0} = -2\,\mathrm{i}\,M\,a^{-2}\,b_{\theta0}\,, \tag{1.125a}$$

$$(c_0 + \mathrm{i}\,c_2\,s^2 - \partial_s^2)\,b_{\theta0} = a\,\Omega'(a)\,b_{r0}\,, \tag{1.125b}$$

where $c_0 = \sigma_2 + M^2/a^2 + K^2$ and $2c_2 = M\Omega''(a) + KU''(a)$. These coupled differential equations can be rewritten as

$$\mathcal{P}_+\mathcal{P}_- b_{r0} = 0\,, \tag{1.126a}$$

with

$$\mathcal{P}_\pm \equiv (c_0 \pm d + \mathrm{i}\, c_2\, s^2 - \partial_s^2), \quad d \equiv (-2\,\mathrm{i}\, M\, \Omega'(a)/a)^{1/2}\,. \tag{1.126b,c}$$

The parabolic cylinder operators $\mathcal{P}_+$ and $\mathcal{P}_-$ commute and so the solution for b_{r0} is a linear combination of solutions to the two equations $\mathcal{P}_\pm b_{r0} = 0$. Putting these into canonical form gives

$$\left[\partial_\sigma^2 - (\tfrac{1}{4}\sigma^2 + c_\pm)\right]\, b_{r0} = 0\,, \tag{1.127}$$

with $$\sigma = s(4\,\mathrm{i}\, c_2)^{1/4}\,, \qquad c_\pm = (c_0 \pm d)/(4\,\mathrm{i}\, c_2)^{1/2}\,, \tag{1.128a,b}$$

and solutions that decay for $s \to \pm\infty$ exist only if $c_\pm = -j - \frac{1}{2}$ for $j = 0, 1, 2, \ldots$. This gives eigenvalues of the original dynamo problem.

Finally returning to the original variables gives leading order growth rates,

$$\gamma \equiv \mathrm{Re}\,\sigma \simeq \mp\sqrt{\varepsilon|m\Omega'(a)|/a} - (j+\tfrac{1}{2})\sqrt{\varepsilon|m\Omega''(a) + kU''(a)} - \varepsilon(m^2/a^2 + k^2)\,. \tag{1.129}$$

This formula was derived for $m, k = \mathcal{O}(\varepsilon^{-1/3})$, but is in fact valid for all m, k. The fastest growing modes have scales $m, k = \mathcal{O}(\varepsilon^{-1/3})$ and $\gamma = \mathcal{O}(\varepsilon^{1/3})$, and so this provides a slow dynamo. The resulting magnetic fields have spiralling tubes along which the field is approximately directed; for example, an $m = 2$ mode is illustrated schematically in Figure 1.11.

An important feature of the formula (1.129) is that the first two terms scale in precisely the same way with m (and k) and ε, while the last term can always be made subdominant at small ε by taking m (and k) small enough. Taking the upper sign, and $j = 0$, for a dynamo to occur at large Rm for some mode (m, k) it follows that the first, positive term must dominate the second, negative term, and this only occurs at the given resonant surface $r = a$ provided the purely geometrical condition, obtained with the help of (1.124a),

$$r\left|\frac{\Omega''(r)}{\Omega'(r)} - \frac{U''(r)}{U'(r)}\right| < 4\,, \tag{1.130}$$

is met there. One can write down flows for which this is not satisfied, and so which would not be dynamos at large Rm, even though they appear well-endowed with helical streamlines.

This example can be generalised away from strictly circular geometry to allow more general stream surfaces (Gilbert & Ponty, 2000). As an example of an application, the resulting theory gives excellent predictions of the instability threshold for these

Ponomarenko modes in a study (Plunian, Marty & Alémany, 1999) of dynamo instabilities in model nuclear reactor flows, even at moderate Rm. Such modes can also occur in convective cellular flows (e.g., Ponty, Gilbert & Soward, 2001). A smooth flow of the form (1.119) can give slow dynamo action, but if $\Omega(r)$ and $U(r)$ have discontinuities at some radius $r = a$, then fast dynamo action can occur, with growth rates $\gamma = \mathcal{O}(1)$ for modes with $m, k = \mathcal{O}(\varepsilon^{-1/2})$ (Gilbert, 1988); we will not discuss this further here. Some aspects of the saturation of smooth Ponomarenko dynamos are studied in Bassom & Gilbert (1997) for $\mathrm{Re} \gg \mathrm{Rm} \gg 1$: the flow adopts a layered structure, with solid body rotation in a broad region surrounding the radius a and where the α–effect and field are concentrated. Outside are thin layers where the shear and ω–effect are significant.

These Ponomarenko modes, with spiralling tubes of field alternating in direction, are rather localised; for example a mode would sit in one cell of a convective flow. They are far from the mean-field dynamos which are traditionally studied by means of an α–effect and discussed in Section 1.5. The best laminar flow to study which allows such large-scale field generation is the Roberts (1970) flow, which was introduced in Section 1.4,

$$\mathbf{u} = (\sin x \cos y, -\cos x \sin y, K \, \sin x \sin y)\,, \qquad K = \sqrt{2}\,. \tag{1.131a,b}$$

This is a Beltrami flow, with vorticity $\boldsymbol{\nabla} \times \mathbf{u} = K\mathbf{u}$ proportional to the flow itself. It thus provides a steady solution to the Euler equation, and is a member of the ABC family of flows; the general ABC flow is given by

$$\mathbf{u} = (C \sin z + B \cos y, A \sin x + C \cos z, B \sin y + A \cos x)\,, \tag{1.132}$$

where A, B and C are parameters (and (1.131a,b) is obtained by setting $A = B = 2^{-1/2}$, $C = 0$, rescaling and rotating axes through $\pi/4$). At low Rm the Roberts flow provides an α–effect dynamo, destabilising large-scale magnetic field modes (e.g., Moffatt, 1978). The field is dominated by diffusion; the flow is a small perturbation to the field on the scales of the flow, but one which has a large-scale destabilising effect. A nonlinear study within this low Rm model reveals an inverse cascade of magnetic energy to large scales (Gilbert & Sulem, 1990).

At large Rm, however, the field tends to localise on stream surfaces. The flow is independent of z; there is an array of square helical cells, in which the flow is spiralling, where dynamos can exist. However the key new feature is the network of hyperbolic stagnation points $(x, y) = (n\pi, m\pi)$, joined by straight-line separatrices: new magnetic modes appear, localised on this network. A mode $\mathbf{B} \propto \exp(\mathrm{i}\, k\, z + \sigma\, t)$ with wavenumber k in z has growth rate

$$\gamma \equiv \sigma = \alpha k - \varepsilon k^2\,, \qquad \alpha = -\tfrac{1}{2} k \varepsilon^{1/2} G\,, \qquad G \simeq 1.0655\,. \tag{1.133a,b,c}$$

(Childress, 1979; Soward, 1987). This is valid for $k = \mathcal{O}(1)$, but the growth rate increases with k, and the above equation is suggestive of a maximum growth rate

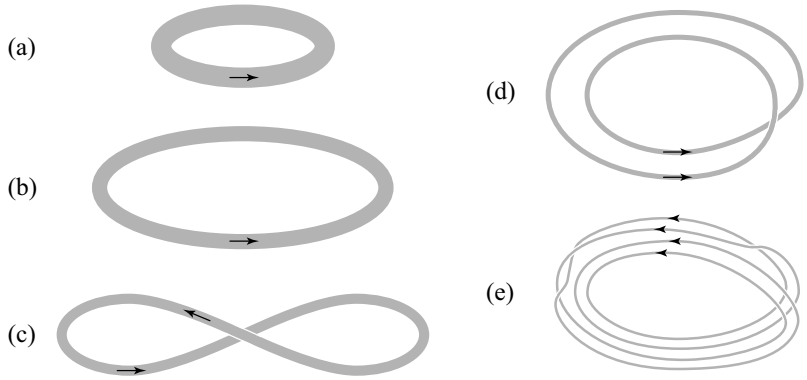

Figure 1.12 - The stretch–twist–fold dynamo: an initial flux tube (a), is stretched (b), twisted (c) and folded (d), to obtain a doubled flux tube. (e) a folded flux tube after two STF cycles: note that only the centre line of the tube is shown.

$\gamma = \mathcal{O}(1)$ for $k = \mathcal{O}(\varepsilon^{-1/2})$, that is, a fast dynamo. A delicate analysis (Soward, 1987) shows that the maximum growth rate is in fact given by

$$\gamma = \mathcal{O}((\log\log\varepsilon^{-1})/\log\varepsilon^{-1})\,, \qquad k = \mathcal{O}(\varepsilon^{-1/2}/\sqrt{\log\varepsilon^{-1}})\,. \qquad \text{(1.134a,b)}$$

Is this a fast dynamo? Not technically, as the growth rate still goes to zero as $\varepsilon \to 0$ and so the dynamo is slow. However the decay is only logarithmic in ε, and what is a logarithm between friends? In view of our opening remarks in this chapter, this is therefore still an interesting and important slow dynamo mechanism; for example, similar Roberts modes are found in the study of Plunian, Marty & Alémany (1999). One important feature to note is that the fastest growing magnetic field modes have a very small lengthscale in z. They are extended in x and y (unlike the Ponomarenko modes), but the magnetic energy is entirely at the diffusive scales, $k \simeq \mathcal{O}(\varepsilon^{-1/2})$. In the Roberts dynamo diffusion is still playing a crucial *rôle* in the amplification process, and the field has to adopt diffusive scales to benefit. This should be contrasted with the fast dynamos below, where the magnetic fields have typically a power-law spread of energy over a range of scales, from the full scale of the flow down to diffusive scales.

1.6.2. THE STRETCH–TWIST–FOLD PICTURE

In so far as finding fast dynamos, the problem with the flows so far discussed is that diffusion is crucially involved in the amplification process. In fact, in rough terms, these steady flows have dynamos of an $\alpha\omega$-type at large Rm. Field perpendicular to stream surfaces is stretched out along stream surfaces by the flow, giving strong field parallel to stream surfaces (an ω–effect); in curved geometry weak diffusion acts

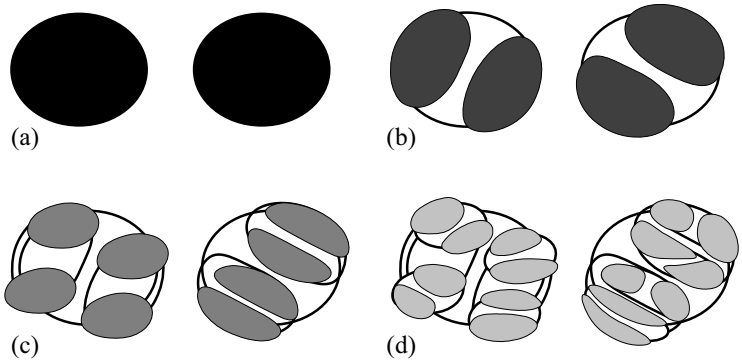

Figure 1.13 - Cross sections of the torus (a) initially, and (b) after one STF iteration, (c) two iterations and (d) three iterations. Shading indicates regions containing field, and white is field-free fluid.

on this parallel field to generate perpendicular field (an α–effect). This $\alpha\omega$-cycle allows the field to grow and the dynamo to operate. To avoid the dynamo process being limited by diffusion as in these examples, it is necessary for advection by the fluid flow to do all the amplification itself without relying on diffusion. The simplest picture of how this may be achieved is in the stretch–twist–fold (STF) dynamo (see Section 1.2.3; Vainshtein & Zeldovich, 1972), depicted in Figure 1.12 (see also Figure 1.2).

In this figure the flow is not given explicitly. Instead the action of the flow is shown on a tube of field frozen into the fluid; we may think of the perfectly conducting case $\varepsilon = 0$ for the moment. The initial tube (a) is stretched to twice its length, its cross section being halved, giving (b). This doubles the field strength and so multiplies the energy by four. The field is then twisted into a figure-of-eight (c) and folded (d), to give a tube of similar structure to the original in (a). If this process is repeated, with a time period $T = 1$, then the energy at time $t = n$ will be $E_n = 2^{2n}E_0$, corresponding to a growth rate $\gamma = \log 2$. Now let us reintroduce weak diffusion; this will begin to play a *rôle* when the field scale becomes of order $\varepsilon^{1/2}$, and will begin to smooth and reconnect the field (Moffatt & Proctor, 1985). Because the action of the STF moves has been to bring tubes of field largely into alignment, one would expect diffusion not to lead to a wholesale destruction of field, but simply to smooth the fine structure in the field, giving $\gamma \simeq \log 2$ for $0 < \varepsilon \ll 1$ and so a fast dynamo with $\gamma_0 \simeq \log 2$.

There are a number of problems with realising the STF picture in practice. The first is that it is not easy to specify a fluid flow to apply the STF moves (Moffatt & Proctor, 1985). But even in such a flow (or iterated mapping), the field rapidly becomes unmanageable (Vainshtein *et al.*, 1996), for the reasons indicated schematically in Figure 1.13. Starting with a magnetic field (black) in a torus, whose cross section

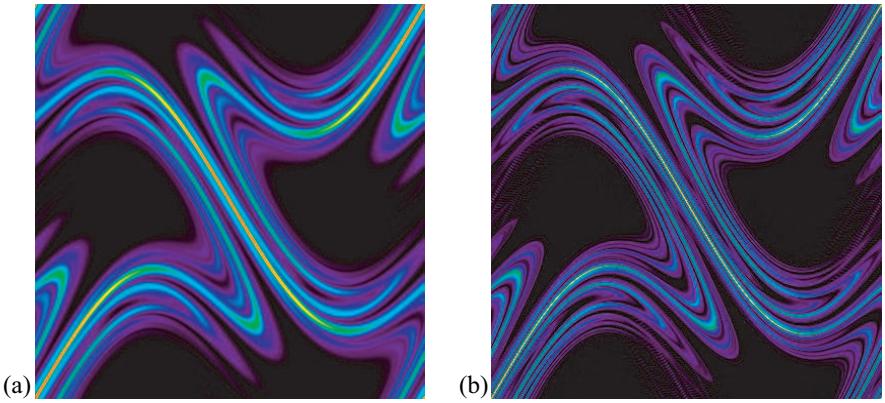

Figure 1.14 - Eigenfunctions of Otani's flow for $k = 0.8$ and (a) $\varepsilon = 5 \times 10^{-4}$ and (b) $\varepsilon = 5 \times 10^{-5}$. The magnitude of the magnetic field is shown, with black indicating zero field. (**See color insert**.)

is shown in (a), the doubled up field in (b) will entrain field-free fluid (white) and so some field will lie outside the original torus. As the stretch, twist, fold operations are repeated (c,d) the bundle of field lines and entrained fluid will increase in volume until the whole fluid volume contains strands of field, and it is necessary to understand the global nature of the fluid flow and folding of field, a problem that has not been addressed. The field lines also become tangled up in a complicated fashion (see Gilbert, 2002), with poorly-understood implications for diffusion of field.

Nonetheless, the STF moves provide a useful picture of how a fast dynamo with growth rate $\gamma_0 \simeq \log 2$ might operate. This is only a *picture*, hard to realise in practice (for example in a convective fluid flow!), but informative nonetheless. The key points to bear in mind are: first, the flow has chaotic particle trajectories, as the length of the field lines in the tube doubles with each period. In fact Lagrangian chaos in a smooth fluid flow is a necessary ingredient for fast dynamo action; technically the topological entropy h of the flow must be positive (Finn & Ott, 1988; Klapper & Young, 1995), as we discuss further below. Such chaotic flows are easy to realise; but the second key ingredient in a fast dynamo is constructive alignment of magnetic field vectors. The STF moves tend to bring fields close with similar orientation, which minimises the possible destruction of field through magnetic diffusion.

1.6.3. FAST DYNAMOS IN SMOOTH FLOWS

The numerical study of dynamo action in chaotic flows began with investigation of steady ABC flows (1.132) (Galloway & Frisch, 1986). However these are generally

three-dimensional, having complex stream line topology, and solving the induction equation is computationally intensive. It is easier to deal with two-dimensional flows $\mathbf{u}(x, y, t)$ (independent of z), and the best-studied examples are essentially variants of (1.131), for which time dependence is introduced and results in a breaking up of the separatrices joining hyperbolic stagnation points, to give chaotic layers. One example is the flow of Otani (1993),

$$\mathbf{u}(x, y, t) = 2\cos^2 t\,(0, \sin x, \cos x) + 2\sin^2 t\,(\sin y, 0, -\cos y)\,, \tag{1.135}$$

which is similar to an example studied by Galloway & Proctor (1992) and discussed in Section 1.4.1. Growing magnetic fields take a Floquet form

$$\mathbf{B}(x, y, z, t) = \mathrm{e}^{\mathrm{i}\,k\,z+\sigma t}\,\mathbf{b}(x, y, t)\,, \tag{1.136}$$

in which $\mathbf{b}$ is periodic in time, period 2π. The z-wave number k is a parameter and for each diffusivity ε, the mode with maximum growth rate may be found. Numerical study (Otani, 1993) shows good evidence for fast dynamo action with

$$\gamma_0 \simeq 0.39\,, \qquad k \simeq 0.8\,. \tag{1.137a,b}$$

Note that the value of k at which growth rates are maximised does not depend on ε; the magnetic field has a large-scale component, unlike in the slow Ponomarenko and Roberts dynamos discussed above.

However while numerical studies show that the convergence of $\gamma(\varepsilon)$ to γ_0 is rapid as $\varepsilon \to 0$, the magnetic eigenfunctions become more and more complicated, as indicated in Figure 1.14. This shows a snapshot of magnetic energy (averaged over z) plotted as a function of (x, y). In the centre are bands of field, resulting from chaotic stretching and folding in the flow in the (x, y)–plane. In the large black, field-free regions the flow has islands of KAM surfaces with insignificant stretching.[3]

The action of the flow is to fold field in the plane, giving the belts of field dominating the centre of the picture. This would not give any kind of constructive alignment of field vectors, however, without the shearing motion in z, which advects field up and down, giving changes of sign of field by virtue of the $\mathrm{e}^{\mathrm{i}\,k\,z}$ dependence on z; see (1.136). By this means bands in the centre of the picture have fields that are largely aligned. This 'stretch–fold–shear' mechanism amplifies a large-scale field component, while creating a cascade of fluctuations to small scales; these fluctuations are smoothed out by diffusion, which plays a relatively passive *rôle*.

While the above flow of Otani (1993) has been written down without any obvious link to real astrophysical fluid flows, the above mechanism of stretching and folding

3 KAM=Kolmogorov-Arnold-Moser: this refers to regions where trajectories are not chaotic and lie on surfaces.

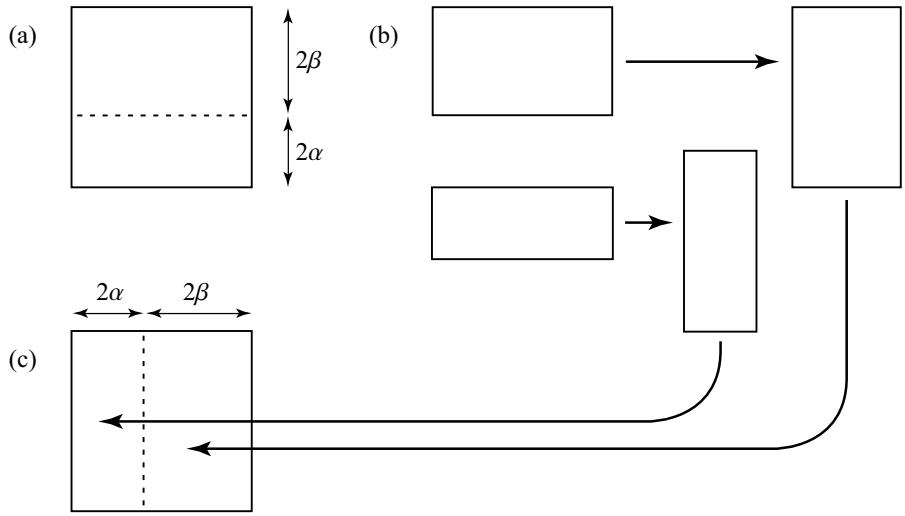

Figure 1.15 - A baker's map with uneven stretching, as described in the text (figure taken from Gilbert 2006).

in the (x, y) plane and shearing in z is very natural and can occur, for example, in convection. Two-dimensional time-dependent convective eddies can give chaotic folding in the plane containing the roll axes, while the influence of rotation (natural in an astrophysical body) can drive flows along their axes (Kim, Hughes & Soward, 1999; Ponty, Gilbert & Soward, 2001).

The flows of Otani (1993) and Galloway & Proctor (1992) have also been studied in dynamical regimes, where the given fluid flow is now driven by a prescribed body force until the field grows and becomes dynamically involved through the Lorentz force. Studies indicate that the field saturates through suppression of the Lagrangian chaos and alpha effect in the flow, although there is also some evidence that an inverse cascade of magnetic energy to large scales may occur in spatially extended systems, on long time-scales; see for example, Maksymczuk & Gilbert (1998) and Cattaneo *et al.* (2002).

1.6.4. FAST DYNAMOS IN MAPPINGS

Studying fast dynamo action in flows such as Otani's above, or an ABC flow, is extremely difficult. The problem is that it is not just the individual Lagrangian trajectories that are important, but how ensembles of trajectories lead to folding of magnetic field. Most progress in understanding has been obtained by studying dynamo action in models for which the fluid flow is replaced by a mapping.

Perhaps the simplest mapping that can be considered is the stacked Baker's map

with uneven stretching (Finn & Ott, 1988): this discontinuous map of a square, say $[-1,1]^2$, to itself is depicted in Figure 1.15. The map M is defined by a parameter α with $0<\alpha<1$ and we set $\beta=1-\alpha$. The unit square is cut at a horizontal level $y=-1+2\alpha$ into two pieces. The first is stretched by a factor α^{-1}, changing its dimensions in (x,y) coordinates from $2\times 2\alpha$ to $2\alpha\times 2$; see (b). The second piece is stretched by a factor β^{-1}, going from $2\times 2\beta$ to $2\beta\times 2$. Finally the two squares are reassembled in (c), stacked together, and this completes the mapping process. This mapping can be thought of as a simplified model for the STF picture, giving the doubling up of the tubes of flux in the presence of uneven stretching (Finn & Ott, 1988). The map M may be written as

$$M(x,y)=\begin{cases}(\alpha(x+1)-1,\alpha^{-1}(y+1)-1) & \text{for } y<\Upsilon\,;\\ (\beta(x-1)+1,\beta^{-1}(y-1)+1) & \text{for } y\geq\Upsilon\,,\end{cases} \tag{1.138}$$

with $\Upsilon=-1+2\alpha\equiv 1-2\beta$.

We imagine starting with a field $\mathbf{B}(x)=b(x)\,\mathbf{e}_y$ and using the Cauchy solution, it may be checked that the action of M is to replace $b(x)$ with the field Tb, where

$$Tb(x)=\begin{cases}\alpha^{-1}b(\alpha^{-1}(x+1)-1) & \text{for } x<\Upsilon\,;\\ \beta^{-1}b(\beta^{-1}(x-1)+1) & \text{for } x\geq\Upsilon\,.\end{cases} \tag{1.139}$$

T is called the dynamo operator (without diffusion). Ignoring diffusion for the present, we may imagine iterating this operator on an initial unit magnetic field $b_0(x)=1$, possessing flux $\Phi_0=2$ through any horizontal line $y=$ constant. Applying the map once yields two rectangles of field, one of width 2α and strength α^{-1}, and one of width 2β, strength β^{-1}: the flux $\Phi_1=4$ has been doubled. Iterating the map we see that $\Phi_n=2^{n+1}$. If we can ignore the effects of diffusion we have a dynamo with growth rate $\gamma_0=\log 2$ as in the STF picture, if we agree that each iteration of the mapping takes unit time. We would expect the effect of weak diffusion to be unimportant, as the fields that emerge through repeated application of M are all pointing in the same direction (Finn & Ott, 1990).

The key feature that the stacked Baker's map highlights is that the rate of growth of flux can be different from the Liapunov exponent, a popular measure of how chaotic a system is. To measure this quantity we imagine how a y-directed vector attached to a typical point (x,y) is stretched as the map M is iterated. Since on average a proportion α of the iterates $M^n(x,y)$ will lie in $y<\Upsilon$, where the vector will be stretched by a factor α^{-1}, and a proportion β in $y>\Upsilon$, with stretching by β^{-1}, the Liapunov exponent will be

$$\lambda_{\text{Liap}}=\alpha\log\alpha^{-1}+\beta\log\beta^{-1}\,. \tag{1.140}$$

This is *less* than the fast dynamo growth rate $\gamma_0=\log 2$, except in the special case $\alpha=\beta=1/2$, of even stretching. This at first seems surprising, as magnetic field

is composed of vectors, and surely both γ_0 and λ_{Liap} measure the stretching rate of vectors! In fact there is a difference in the averaging processes involved. In the case of magnetic field, in computing a flux, we are weighting more heavily the more stretched vectors, by integrating $b(x)\,dx$, whereas a Lipaunov exponent involves a *typical* point, with weighting dx in the sense of a measure. Equivalently, stronger magnetic fields tend to concentrate in the regions of higher stretching, and so give a different weight in the average.

A more useful quantity to measure as a diagnostic in a fast dynamo is the rate of stretching h_{line} of material lines (which could be thought of as field lines in the absence of diffusion). If the reader experiments with placing a line, say $x = y$ in the square $[-1, 1]^2$ (see Figure 1.15), and then iterating the map M on all the points constituting the line, he or she will soon find that the line length approximately doubles with each iteration, giving an asymptotic value $h_{\text{line}} = \log 2$, which is the same as the fast dynamo growth rate γ_0. Like magnetic field, material lines tend to concentrate in the regions of high stretching (with the consequent inequality $\lambda_{\text{Liap}} \leq h_{\text{line}}$).

This then suggests the general result that the fast dynamo exponent γ_0 should not exceed h_{line}. In fact in two dimensions the exponent h_{line} may be identified with the topological entropy h, and so the result one might expect is

$$\gamma_0 \leq h\,; \tag{1.141}$$

this was argued by Finn & Ott (1988) and proved rigorously (under some natural smoothness conditions) by Klapper & Young (1995). The fact that γ_0 can be less than h is easily understood: the Baker's map in (1.138) above gives perfect alignment of field in the vertical: all vectors point in the $+y$ direction with our given initial condition. If instead there is folding of field in a more realistic scenario, which can be modelled using a Baker's map with several cuts and rotating one or more rectangles of field at each iteration, the flux Φ_n, a signed quantity, will tend to grow less quickly than the rate of stretching of material lines. This aspect can also be characterised by a *cancellation exponent* (Du *et al.*, 1994). If there are no sign changes in the field, the cancellation exponent would be zero, and we would have $\gamma_0 = h$.

While the uneven Baker's map model is an interesting and useful way to explore these considerations of uneven stretching and cancellations, it suffers from the fact that it is derived from the STF picture, which has the shortcomings and problems mentioned above. Note that for $\alpha = \beta = 1/2$ the Baker's map is trivial (doubling all field vectors and no cancellations), and so probably too simple to model what occurs in a typical fluid flow!

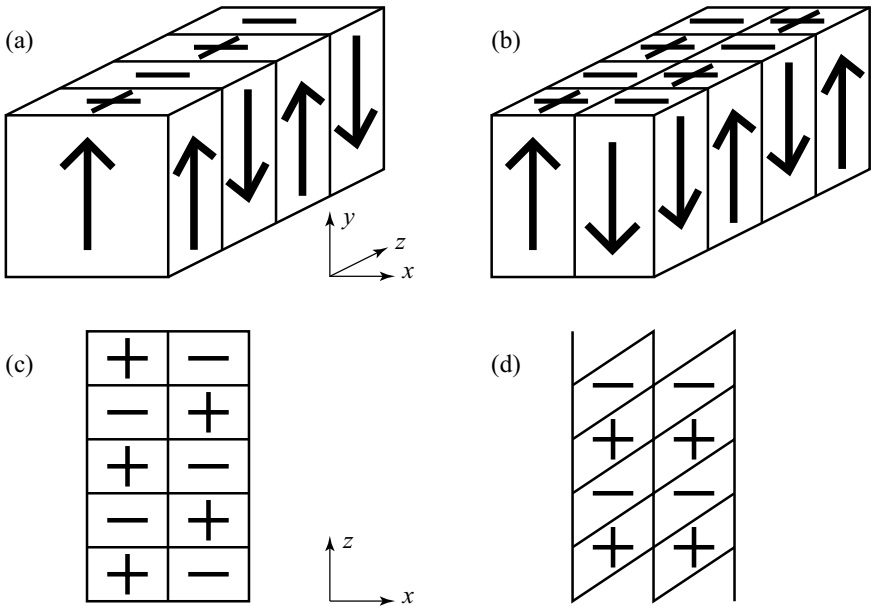

Figure 1.16 - The stretch–fold–shear map. (a) Magnetic field depending on z is stretched and folded with a Baker's map in the (x, y)–plane to give (b). In (c) the field orientation is shown in the (x, z)–plane, which after the shear operation gives (d) (figure taken from Gilbert, 2002).

1.6.5. THE STRETCH–FOLD–SHEAR MODEL

Another idealised model that does capture some of the amplification mechanism seen in Otani's (1993) flow and similar flows, is the stretch–fold–shear (SFS) model of Bayly & Childress (1988, 1989). This model consists of a number of components. The first is a folded Baker's map (with uniform stretching), which maps the square $-1 \le x, y \le 1$ to itself, by stretching and folding. This is like the process depicted in Figure 1.15 with $\alpha = \beta = 1/2$, except that the second rectangle is rotated through π before reassembly, representing the folding of a sheet of field. The map is defined by

$$M_1(x,y,z) = \begin{cases} (\frac{1}{2}(x-1), 1+2y, z) & \text{for } y < 0\,; \\ (\frac{1}{2}(1-x), 1-2y, z) & \text{for } y \ge 0\,. \end{cases} \tag{1.142}$$

The action of this on a magnetic field

$$\mathbf{B}(x,y,z) = \mathrm{e}^{\mathrm{i}\,k\,z} b(x)\,\mathbf{e}_y + \text{complex conjugate} \tag{1.143}$$

is shown in Figure 1.16(a,b), giving one fold of field in the (x,y)–plane. If this map were now simply repeated, the effect would be to obtain ever finer alternating bands of magnetic field in this plane, vulnerable to diffusion. There is plenty of stretching, but no constructive folding. The flux through a line $x =$ constant would become zero after one iteration and remain so thereafter. In this case we would have γ_0 negative, but $h_{\text{line}} = \log 2$.

Thus a second ingredient is required, a shear in the z-direction, shown in a top-down view going from (c) to (d). The action of the shear is to bring upward pointing field ($+$) approximately into alignment with other upward fields, and similarly downward pointing field ($-$). This corresponds to the mapping

$$M_2(x,y,z) = (x, y, z + \alpha x)\,, \tag{1.144}$$

where α is a shear parameter (not related to the previous α, and not intended to imply an α–effect!). The alignment is only approximate, but intended to capture the basic mechanism observed in flows such as Otani's, in which belts of field are drawn out and folded in the (x,y)–plane, and then sheared in the z-direction (Bayly & Childress, 1988).

In this way we obtain the SFS dynamo model: the field is first stretched and folded (by M_1) and then sheared (by M_2). Acting on the complex field $b(x)$ in (1.143) above gives a field Tb, with

$$Tb(x) = \begin{cases} 2\mathrm{e}^{-\mathrm{i}\,\alpha\,k\,x}\, b(1+2x) & \text{for } x < 0\,; \\ -2\mathrm{e}^{-\mathrm{i}\,\alpha\,k\,x}\, b(1-2x) & \text{for } x \ge 0\,. \end{cases} \tag{1.145}$$

T is again the dynamo operator without diffusion. For diffusion we employ suitable boundary conditions and allow the field $b(x)$ to diffuse for unit time according to $\partial_t b = \varepsilon \partial_{xx} b$. Possible boundary conditions (only employed at $x = -1, 1$) include insulating (I), perfectly conducting (C) and periodic (P),

$$b(1) = b(-1) = 0 \quad \text{(I)}\,, \quad \partial_x b(1) = \partial_x b(-1) = 0 \quad \text{(C)}\,, \quad b(x) \text{ periodic} \quad \text{(P)}\,. \tag{1.146a,b,c}$$

The diffusion step may be written as mapping b to $H_\varepsilon b$, where H_ε is another operator involving heat kernels (for further details see Gilbert, 2002, 2004).

Finally the SFS dynamo operator with diffusion is written $T_\varepsilon = H_\varepsilon T$. The magnetic field is most easily discretised using Fourier series, and eigenvalues λ for $T_\varepsilon b = \lambda b$ sought numerically using matrix eigenvalue solvers. If the mapping and diffusion are assumed to take a time unity, then the corresponding magnetic growth rate is

$$\sigma = \log \lambda\,, \tag{1.147}$$

and we refer to λ as the growth factor. An eigenvalue λ then corresponds to a growing magnetic mode provided that $|\lambda| > 1$. Our aim is to understand the properties of eigenvalues of T_ε in the limit as $\varepsilon \to 0$. If eigenvalues remain bounded above $|\lambda| = 1$ in the limit, then the SFS model is a fast dynamo.

Figure 1.17(a,b,c) shows the modulus $|\lambda|$ of the leading eigenvalues λ as a function of α (with $k = 1$ set without loss of generality) for the (I), (C) and (P) boundary conditions given above, at $\varepsilon = 10^{-5}$. We see that it is necessary in all cases to increase the shear parameter α above about $\pi/2$ to obtain growing modes. There has to be sufficient constructive alignment for the dynamo to operate.

We also see that the modes with the larger values of $|\lambda|$, certainly $|\lambda| > 1$, are robust to the kinds of boundary condition employed, though the picture is rather different for marginal and decaying modes with $|\lambda| \leq 1$. Further numerical study (not set out here) indicates that the more robust eigenvalues, with $|\lambda| > 1$, appear to show convergence to positive values as $\varepsilon \to 0$, although individual magnetic modes $b(x)$ show increasingly fine structure in this limit. Thus there is good evidence for fast dynamo action in the SFS model (Bayly & Childress, 1988, 1989).

This leaves open the mathematical question: how can we prove fast dynamo action, and obtain some information about these growth rates for small positive diffusivity, $0 < \varepsilon \ll 1$? We need to set out a sensible problem for zero diffusion, and then treat diffusion as a perturbation. The key idea of Bayly & Childress (1989) is to note that while the (diffusionless) operator T tends to reduce the scales of a magnetic field and generally has no eigenfunctions, its adjoint T^* (in L^2), given by

$$T^* c(x) = \mathrm{e}^{-\mathrm{i}\,\alpha\,\frac{1}{2}(x-1)} c\left(\tfrac{1}{2}(x-1)\right) - \mathrm{e}^{-\mathrm{i}\,\alpha\,\frac{1}{2}(1-x)} c\left(\tfrac{1}{2}(1-x)\right)\,, \tag{1.148}$$

instead tends to expand scale and average. T^* can possess smooth eigenfunctions even at zero diffusion, unlike T.

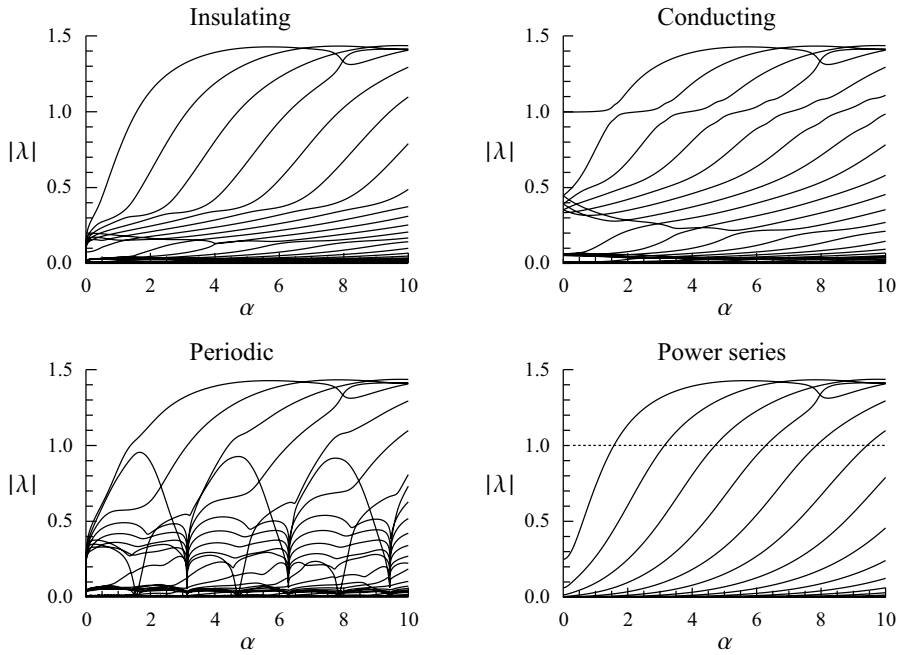

Figure 1.17 - Moduli of eigenvalues $|\lambda|$ plotted against α for the SFS model. The boundary conditions are (a) insulating, (b) perfectly conducting and (c) periodic, with $\varepsilon = 10^{-5}$. In (d) eigenvalues are obtained using a power series and $\varepsilon = 0$.

If we seek an eigenfunction $T^*c = \lambda c$, and expand the function $c(x)$ in a basis x^n, that is as a power series about the origin, we obtain a matrix for T^* whose eigenvalues may be found numerically. Figure 1.17(d) gives growth factors obtained in this way for zero diffusion. The results are very close to those obtained in Figure 1.17(a,b,c) in the presence of weak diffusion, particularly for larger values of $|\lambda|$. Plainly most branches in Figure 1.17(d) are relatively robust to diffusion, though this depends on boundary conditions and the size of $|\lambda|$.

One branch that shows particular sensitivity to diffusion and boundary conditions is the horizontal branch in 1.17(d), for which the adjoint eigenfunction of (1.148) is given analytically by

$$c(x) = \mathrm{e}^{\mathrm{i}\,\alpha\,(x-1)} - \mathrm{e}^{\mathrm{i}\,\alpha\,(1-x)} = 2\,\mathrm{i}\,\sin\alpha(x-1)\,, \quad \lambda = \mathrm{e}^{\mathrm{i}\,\alpha}\,. \tag{1.149a,b}$$

This branch only survives for conducting boundary conditions. Current research (Gilbert, 2004) is aimed at understanding the effects of diffusion and boundary conditions in the SFS model. The aim is to be able to use perturbation theory to write, for a given branch and value of α,

$$\lambda(\varepsilon) \simeq \lambda(0) + C\varepsilon^q\,, \tag{1.150}$$

where $\lambda(0)$ is the complex growth factor obtained by means of a power series for zero diffusion, as shown in Figure 1.17(d). The term $C\varepsilon^q$ is the diffusive correction, which is dependent on the structure of the mode and boundary conditions, and $q > 0$ is the condition on the exponent q for the branch to survive the effects of diffusion.